ELECTROMAGNETIC WAVE PROPAGATION

Fernando L. Teixeira[1], Fernando J. S. Moreira[2], and Odilon M. C. Pereira-Filho[3]

[1] *The Ohio State University, Columbus, Ohio*
[2] *Federal University of Minas Gerais, Belo Horizonte, Brazil*
[3] *Federal University of Pernambuco, Recife, Brazil*

1 INTRODUCTION

1.1 Historical Perspective

Electromagnetic waves play a major role in remote sensing and communication systems. The equations governing electromagnetic wave propagation were first established by J. C. Maxwell (1831–1879) in 1864 [1]. However, one should not overlook previous contributions of many scientists over the centuries, especially in optics. Speculations regarding the nature of light date since Ancient Greece, when philosophers were already acquainted with the rectilinear propagation, reflection, and refraction of light [2]. The major contributions to the field, however, initiated during the Renaissance, on the foundations of the experimental method introduced by Galileo (1564–1642). Some examples are the law of refraction discovered by Snell (1580–1626) in 1621, the principle of least time established by Fermat (1601–1665) in 1657, the observation of light diffraction by Grimaldi (1618–1663) and Hooke (1635–1703) circa 1665, and Huygen's (1629–1695) envelope construction (leading to the principle named after him) in 1678 [2]. Such observations and experiments lead the development of a wave theory to explain the nature of light as luminous sources vibrating in adjacent portions of an ethereal medium, an interpretation similar to that of acoustic waves. The wave theory of light was, however, later rejected by Newton (1642–1727), who proposed a corpuscular interpretation instead [2].

Many years passed away until new experiments reinforced the wave theory of light. Among the leading scientists responsible for that is Fresnel (1788–1827), who developed the theory of light reflection and refraction in a more quantitative way and as well as a firmer mathematical basis for the interpretation of light as a transverse wave. Fresnel's work temporarily obscured the corpuscular theory of light, which regained strength only after Planck's (1858–1947) and Einstein's (1879–1955) started to unveil the quantum aspects of light in the beginning of the 1900's. The nineteenth century also witnessed the efforts of many physicists to experimentally determine the speed of light, such as Michelson (1852–1931).

Apart from the developments in optics, many scientists dedicated efforts to establish the physical nature of magnetism and electricity. Among then, it is worth mentioning Coulomb (1736–1806), who demonstrated the inverse square law for electrical forces in 1785, Oersted (1777–1851), who was perhaps the first to observe

Update based on the previous version of this chapter by Fernando L. Teixeira, Fernando J. S. Moreira, and Odilon M. C. Pereira-Filho, *Encyclopedia of RF and Microwave Engineering*, © 2005, John Wiley & Sons, Inc.

Encyclopedia of RF and Microwave Engineering, Second Edition. Edited by Christopher T. Rodenbeck.

DOI: 10.1002/0471654507.erfme029

experimentally the effect of electrical currents upon the magnetic field in 1820, and Ampère (1775–1836), who formulated the circuit force law and postulated magnetism as an electrical phenomenon. The milestone experiment for the unification of magnetism and electricity, however, was carried out by Faraday (1791–1867), who discovered electromagnetic induction in 1831. The electromagnetic theory known at that time was put on analytical ground by Maxwell (1831–1879) in 1955–1956. He further developed a model to explain electromagnetics as a mechanical phenomenon, which lead into the concept of displacement currents and the consequent generalization of Ampère's law in 1961. The mechanical model was finally abandoned and Maxwell, in 1964, published his third paper on the subject, establishing the basis of the electromagnetic theory [1]. Besides postulating the displacement current, Maxwell was the first to predict the propagation of electromagnetic waves and to postulate light itself as an electromagnetic radiation. This provoked strong opposition from scientists at that time, as no evidence of such waves had been observed by experiments.

Maxwell did not survive to see his ideas been accepted by the majority of the scientists, which just came after the first experimental observation of electromagnetic wave propagation by Hertz, published in 1888. After that, the use of electromagnetic waves for practical purposes was just a matter of time, and in 1901 Marconi (1874–1937) achieved the first transmission of radio signals across the Atlantic. Today, electromagnetic waves permeate most of modern technologies.

In this chapter, we will discuss fundamental aspects of the electromagnetic wave propagation in a somewhat cursory fashion. Further details on this vast subject can be found in several books, such as [2–12].

1.2 The Electromagnetic Wave Spectrum

Since electromagnetic waves can propagate over vastly different frequencies and it is therefore customary to classify electromagnetic waves according to their frequency range. The IEEE frequency band designations are:

- 3–30 Hz: EFL (extra-low-frequency) waves.
- 30–300 Hz: SLF (super-low-frequency) waves.
- 300 Hz –3 kHz: ULF (ultra-low-frequency) waves.
- 3–30 kHz: VLF (very low-frequency) waves.
- 30 –300 kHz: LF (low-frequency or long) waves.
- 300 kHz–3 MHz: MF (medium-frequency or medium) waves, which include most AM radio waves.
- 3–30 MHz: HF (high-frequency or short) waves, which include most of short wave radio.
- 30–300 MHz: VHF waves, which include FM radio and some over-the-air TV signals.
- 300 MHz–3 GHz: UHF waves, which include TV signals, radar waves at L- and S-bands, GPS signals, and microwave oven radiation.
- 3–30 GHz: SHF (centimeter) waves, which include radars at C-, X-, Ku-, and K-bands, some satellite communication links, and aircraft landing systems.
- 30–300 GHz: EHF (millimeter) waves, which include radars at Ka-band, collision avoidance radars, and high-speed microwave data links.

For an electromagnetic wave propagating in air or vacuum, the wavelength λ and frequency f are related by $\lambda = c/f$, where $c \approx 3 \times 10^8$ m/s is the speed of light in vacuum. Therefore, electromagnetic waves can also be classified according to their wavelength. Microwaves correspond to electromagnetic waves with λ from around 1 cm to 1 m (300 MHz $\sim$ 30 GHz). Millimeter and submillimeter waves have λ around 1 mm to 1 cm (30 GHz $\sim$ 300 GHz) and just below it, respectively. Visible light is a form of electromagnetic wave with λ from about 0.38 to about 0.74 μm. Wavelengths just below visible light correspond to ultraviolet waves, while at wavelengths just above visible light correspond to near-infrared waves to about 1.3 μm and thermal infrared waves to about 15 μm. At even smaller wavelengths (higher frequencies) one encounters X-rays and gamma rays [10].

2 MAXWELL'S EQUATIONS AND THE WAVE EQUATION

The propagation of electromagnetic waves is governed by Maxwell's equations, which in SI units and for macroscopic field quantities are [13]

$$\begin{aligned} \nabla \times \boldsymbol{\mathcal{E}} &= -\frac{\partial \boldsymbol{\mathcal{B}}}{\partial t} & \nabla \cdot \boldsymbol{\mathcal{D}} &= q \\ \nabla \times \boldsymbol{\mathcal{H}} &= \boldsymbol{\mathcal{J}} + \frac{\partial \boldsymbol{\mathcal{D}}}{\partial t} & \nabla \cdot \boldsymbol{\mathcal{B}} &= 0 \end{aligned} \tag{1}$$

These four equations are supplemented by *constitutive relations* that relate $\boldsymbol{\mathcal{D}}$ and $\boldsymbol{\mathcal{B}}$ to $\boldsymbol{\mathcal{E}}$ and $\boldsymbol{\mathcal{H}}$. We shall assume propagation in *simple media*, with vacuum as a special case. Simple media stands here for linear, homogeneous, and isotropic materials, which will be assumed lossless for the time being. The constitutive relations in this case write as [13]

$$\boldsymbol{\mathcal{D}} = \varepsilon \boldsymbol{\mathcal{E}} \quad \text{and} \quad \boldsymbol{\mathcal{B}} = \mu \boldsymbol{\mathcal{H}} \tag{2}$$

where ε is the permittivity ($\varepsilon = \varepsilon_o \approx 8.85418782 \times 10^{-12}$F/m in vacuum) and μ is the permeability ($\mu = \mu_o = 4\pi \times 10^{-7}$H/m in vacuum), constant scalar numbers for simple media. The electric current $\boldsymbol{\mathcal{J}}$ and charge density q can be interpreted as the sources of the electromagnetic field and are related to each other by the *continuity equation*:

$$\nabla \cdot \boldsymbol{\mathcal{J}} = -\frac{\partial q}{\partial t} \tag{3}$$

which is implicit in (1) [13]. From (1), one can also derive a law for the conservation of electromagnetic energy, the *Poynting's theorem* [13]. For our purposes, we just need to emphasize the *Poynting's vector*, defined as

$$\boldsymbol{\mathcal{S}} = \boldsymbol{\mathcal{E}} \times \boldsymbol{\mathcal{H}} \tag{4}$$

This vector gives the magnitude and direction of power flow density (Watts per meter square).

We will discuss the relations between causative sources ($\boldsymbol{\mathcal{J}}$ and q) and fields ($\boldsymbol{\mathcal{E}}$ and $\boldsymbol{\mathcal{H}}$) later on. For now, we shall only investigate simple characteristics of the electromagnetic propagation. In regions of a simple media where no source is present (i.e., $\boldsymbol{\mathcal{J}} = q = 0$), the (homogeneous) *wave equations* below can be derived from (1) [13]:

$$\begin{aligned} \nabla^2 \boldsymbol{\mathcal{E}} - \frac{1}{c^2} \frac{\partial^2 \boldsymbol{\mathcal{E}}}{\partial t^2} &= 0 \\ \nabla^2 \boldsymbol{\mathcal{H}} - \frac{1}{c^2} \frac{\partial^2 \boldsymbol{\mathcal{H}}}{\partial t^2} &= 0 \end{aligned} \tag{5}$$

where $c = 1/\sqrt{\mu\varepsilon}$ is the *speed of light* in the medium ($c = c_o = 299{,}792{,}458$ m/s in vacuum, by definition). From (5), one can readily show that each Cartesian component of $\boldsymbol{\mathcal{E}}$ and $\boldsymbol{\mathcal{H}}$ also satisfies the following homogeneous (scalar) wave equation:

$$\nabla^2 \psi - \frac{1}{c^2} \frac{\partial^2 \psi}{\partial t^2} = 0 \tag{6}$$

where ψ represent one of such components. The wave equation governs the behavior of ψ with respect to both position (x, y, z) and time (t). For simplicity, let us consider a one-dimensional problem (i.e., no variations on x or y), such that (6) simplifies to

$$\frac{\partial^2 \psi}{\partial z^2} - \frac{1}{c^2} \frac{\partial \psi}{\partial t} = 0 \tag{7}$$

It can be easily verified that a solution to (7) is

$$\psi = f(z - ct) + g(z + ct) \tag{8}$$

where f and g are square-integrable and twice-differentiable, but otherwise arbitrary functions [14]. These solutions are called *D'Alembert's solutions*, where $f(z - ct)$ represents a generic waveform propagating in the

positive z direction with speed equal to c, while $g(z - ct)$ represents another generic waveform with same speed but propagating in the negative z direction.

Although (8) represents the solution of an idealized problem, it illustrates a fundamental property of the solutions of (6): for unbounded simple media, they represent traveling waves which propagate with speed c. In real-life situations, obstacles (ground, vegetation, man-made constructions, etc.) are often present and impose additional constraints (*boundary conditions*) on the solutions of (6), but this fundamental property still holds. In general, the presence of obstacles complicates the problem and simple analytical solutions can only be found for simple geometries. Otherwise, the solutions to (6) can be computed by numerical methods [15–17].

2.1 Time-Harmonic Regime

Most radiofrequency (RF) and microwave applications deal with time-invariant linear media [6]. In this case, the use of a time-harmonic representation is mathematically more convenient to deal with electromagnetic wave phenomena. Assuming a $e^{j\omega t}$ time variation, where ω is the angular frequency, Maxwell's equations (1) are rewritten as [6]

$$\begin{aligned} \nabla \times \boldsymbol{E} &= -j\omega \boldsymbol{B} \qquad & \nabla \cdot \boldsymbol{D} &= \rho \\ \nabla \times \boldsymbol{H} &= \boldsymbol{J} + j\omega \boldsymbol{D} \qquad & \nabla \cdot \boldsymbol{B} &= 0 \end{aligned} \tag{9}$$

where the vector fields in (9) are now functions of spatial coordinates only and correspond to complex phasor representations of the original fields in (1), according to

$$\boldsymbol{\mathcal{E}} = \mathfrak{Re}\left(\boldsymbol{E} e^{j\omega t}\right) \tag{10}$$

where $\mathfrak{Re}$ denotes the real part. A similar relation holds for the other fields (and sources). In simple media and using (2), the constitutive relations then become

$$\boldsymbol{D} = \varepsilon \boldsymbol{E} \quad \text{and} \quad \boldsymbol{B} = \mu \boldsymbol{H} \tag{11}$$

The wave equations (5) also assume a simpler representation [6]:

$$\begin{aligned} \nabla^2 \boldsymbol{E} + k^2 \boldsymbol{E} &= 0 \\ \nabla^2 \boldsymbol{H} + k^2 \boldsymbol{H} &= 0 \end{aligned} \tag{12}$$

known as the (homogeneous) *Helmholtz equations*, where $k = \omega\sqrt{\mu\varepsilon}$ is the *wave number*.

It is useful to define *time-average* quantities when dealing with time-harmonic fields. For instance, from (4) and the definition in (10), one can define the *complex Poynting's vector*

$$\boldsymbol{S} = \frac{1}{2} \boldsymbol{E} \times \boldsymbol{H}^* \tag{13}$$

The real part of the complex Poynting vector represents the time average of $\boldsymbol{S}$ [4]. Equation (13) stresses an important characteristic of electromagnetic wave propagation: in-phase components of $\boldsymbol{E}$ and $\boldsymbol{H}$ contribute to $\mathfrak{Re}(\boldsymbol{S})$, representing the *power density* propagating in the direction of $\mathfrak{Re}(\boldsymbol{S})$ [6]; on the other hand, components of $\boldsymbol{E}$ and $\boldsymbol{H}$ in phase quadrature contribute to the imaginary part of $\boldsymbol{S}$, representing a (stationary) *reactive power* density.

In the time harmonic regime, (7) becomes

$$\frac{d^2\Psi}{dz^2} + k^2 \Psi = 0 \tag{14}$$

where Ψ is the complex representation of ψ according to (10). A generic solution of (14) is

$$\Psi = p_1 e^{j(kz+\phi_1)} + p_2 e^{-j(kz+\phi_2)} \tag{15}$$

where p_1 and p_2 are arbitrary complex-valued constants. Consequently, from (10) and observing that for simple media $k = \omega/c$,

$$\psi = p_1 \cos\left[k(z+ct) + \phi_1\right] + p_2 \cos\left[k(z-ct) + \phi_2\right] \tag{16}$$

which is a particular time-harmonic solution of (7) and (8) known as a *plane wave*.

3 PLANE, TEM, AND STATIONARY WAVES

The plane wave is the simplest solution of the homogeneous wave equation. Many important properties of electromagnetic wave propagation can be inferred from this fundamental solution. Moreover, an arbitrary electromagnetic wave in sourceless linear media can be decomposed in terms of plane waves ($e^{\pm jkz}$ in one dimension) in a manner similar to the decomposition of a time domain signal in terms of its spectral components $e^{j\omega t}$ [18].

The complex representation of a plane wave in (15) specifies an amplitude (p) and phase ($kz + \phi$). Moreover, since Ψ represents a Cartesian component of $\boldsymbol{E}$ or $\boldsymbol{H}$, it also indicates the orientation (i.e., the *polarization*) of the vector field.

The plane-wave solution of Ψ in three-dimensions is written as $e^{-j(k_x x + k_y y + k_z z)}$, where $k_{x,y,z}/k$ can be understood as the cosine directors of the wavefront. By defining the *propagation vector* $\boldsymbol{k} = k_x\hat{\boldsymbol{x}} + k_y\hat{\boldsymbol{y}} + k_z\hat{\boldsymbol{z}}$ and putting the components of $\boldsymbol{E}$ and $\boldsymbol{H}$ back together, we arrive at a more general expression for plane waves [6]:

$$\boldsymbol{E} = \boldsymbol{E_o} e^{-j\boldsymbol{k}\cdot\boldsymbol{r}} \quad \text{and} \quad \boldsymbol{H} = \boldsymbol{H_o} e^{-j\boldsymbol{k}\cdot\boldsymbol{r}} \tag{17}$$

where $\boldsymbol{r} = x\hat{\boldsymbol{x}} + \hat{\boldsymbol{y}} + z\hat{\boldsymbol{z}}$ denotes the observation point, and amplitudes and phases of each component are incorporated in the constant complex vectors $\boldsymbol{E_o}$ and $\boldsymbol{H_o}$ (which also determine the wave polarization). Substituting (17) into (12), one obtains the *characteristic equation* or *dispersion relation* (for simple media):

$$k^2 = \omega^2\mu\varepsilon = k_x^2 + k_y^2 + k_z^2 \tag{18}$$

The plane-wave relations for $\boldsymbol{E}$ and $\boldsymbol{H}$ in simple media are obtained by substituting (11), (17), and (18) into (9) with no sources present:

$$\begin{aligned} \boldsymbol{k}\times\boldsymbol{E} &= \omega\mu\boldsymbol{H} & \boldsymbol{k}\cdot\boldsymbol{E} &= 0 \\ \boldsymbol{k}\times\boldsymbol{H} &= -\omega\varepsilon\boldsymbol{E} & \boldsymbol{k}\cdot\boldsymbol{H} &= 0 \end{aligned} \tag{19}$$

Note that $k_{x,y,z}$ can be complex and still satisfy (18). Consequently, it is useful to regard $\boldsymbol{k}$ as a complex vector:

$$\boldsymbol{k} = \boldsymbol{\beta} - j\boldsymbol{\alpha} \tag{20}$$

where $\boldsymbol{\alpha}$ and $\boldsymbol{\beta}$ are real vectors [6]. Since both $\boldsymbol{\alpha}$ and $\boldsymbol{\beta}$ are real, they can be interpreted geometrically in a simple way. Substituting (20) into (17), one verifies that the plane-wave spatial variation in complex notation is of the form $e^{-\boldsymbol{\alpha}\cdot\boldsymbol{r}} e^{-j\boldsymbol{\beta}\cdot\boldsymbol{r}}$, representing the variations of the amplitude (first term) and phase (second one) of the wave as it propagates through the medium. Consequently, the constant amplitude and phase surfaces are planes (hence the name plane waves), with $\boldsymbol{\alpha}$ and $\boldsymbol{\beta}$ pointing to their normal directions, respectively. If such planes coincide (i.e., $\boldsymbol{\alpha} \| \boldsymbol{\beta}$), then the plane wave is denoted as a *uniform* plane wave. Otherwise, it is denoted as *nonuniform*. Furthermore, $\hat{\boldsymbol{\beta}}$ (i.e., unit normal vector to the equiphase surface) denotes the *direction of propagation* of the plane wave.

For uniform plane waves, one can show from (18) and (20) that $\boldsymbol{k} = k\hat{\boldsymbol{k}}$, where $\hat{\boldsymbol{k}} = \hat{\boldsymbol{\beta}}$ is the direction of propagation. Now $\boldsymbol{k}$ has a geometrically defined direction and one can inspect from (19) that Ampère's and Faraday's laws reduce to

$$\boldsymbol{H} = \frac{k}{\omega\mu}\hat{\boldsymbol{k}}\times\boldsymbol{E} = \frac{1}{\eta}\hat{\boldsymbol{k}}\times\boldsymbol{E}$$

$$\boldsymbol{E} = \frac{-k}{\omega\varepsilon}\hat{\boldsymbol{k}} \times \boldsymbol{H} = -\eta\hat{\boldsymbol{k}} \times \boldsymbol{H} \tag{21}$$

where $\eta = \sqrt{\mu/\varepsilon}$ is the *intrinsic impedance* of the medium ($\eta = \eta_o \approx 376.730313\ \Omega$ in vacuum). So, a uniform plane wave has $\boldsymbol{E}$, $\boldsymbol{H}$, and $\hat{\boldsymbol{k}}$ mutually orthogonal to each other (which is not the case for nonuniform plane waves). Waves with such characteristics, that is, obeying the relations in (21), are called *transverse electromagnetic* (TEM) waves, being the plane wave its simplest example.

3.1 Wavelength and Phase Velocity

For simplicity, let us consider a uniform plane wave propagating in the $\hat{\boldsymbol{k}} = \hat{\boldsymbol{z}}$ direction. Consequently, $\boldsymbol{k} \cdot \boldsymbol{r} = kz$. Since $\hat{\boldsymbol{k}} \cdot \boldsymbol{E} = 0$, let us further consider $\boldsymbol{E} = E_o e^{-jkz}\hat{\boldsymbol{x}}$ with $E_o = pe^{j\phi}$. Consequently, from (21), $\boldsymbol{H} = (E_o/\eta)e^{-jkz}\hat{\boldsymbol{y}}$. Note that this is a one-dimensional problem, that is, the components of $\boldsymbol{E}$ and $\boldsymbol{H}$ satisfy (14), with constant amplitude and phase planes perpendicular to $\hat{\boldsymbol{z}}$.

To obtain corresponding expressions in time domain, we apply the definition in (10):

$$\begin{aligned}\boldsymbol{\mathcal{E}} &= p\cos(\omega t - kz + \phi)\hat{\boldsymbol{x}}\\ \boldsymbol{\mathcal{H}} &= (p/\eta)\cos(\omega t - kz + \phi)\hat{\boldsymbol{y}}\end{aligned} \tag{22}$$

So, for a certain instant of time, the spatial variation of $\boldsymbol{\mathcal{E}}$ and $\boldsymbol{\mathcal{H}}$ is sinusoidal with a period equal to $\lambda = 2\pi/k$, the *wavelength* of the electromagnetic wave. Since $k = \omega/c$, then

$$\lambda = c/f \tag{23}$$

where f is the frequency. For such sinusoidal variation, $\omega/k = c$ is called the *phase velocity* (v_p) of the TEM wave.

3.2 Polarization

In the previous example, we have assumed $\boldsymbol{E} \| \hat{\boldsymbol{x}}$; but any combination between x- and y-components also satisfies $\hat{\boldsymbol{k}} \cdot \boldsymbol{E} = 0$ for $\hat{\boldsymbol{k}} = \hat{\boldsymbol{z}}$. In this situation, such components are said to be *orthogonal* to each other and their phase and amplitude relationships describe the nature of the wave polarization. Wave polarization plays an important role in RF and microwave systems, as the interaction between fields and obstacles can strongly depend on it. In principle, it is possible to transmit and receive orthogonal polarizations in a communication channel independently, thus doubling the capacity of the channel. In practice, *depolarization* effects (partial conversion of energy in one polarization to another) often occur. Orthogonal polarizations can also be used in certain radio links to minimize co-channel interference [19].

According to (21), the TEM wave polarization is fully characterized by just $\boldsymbol{E}$ and $\hat{\boldsymbol{k}}$. So, let us assume $\boldsymbol{E} = (p_x e^{j\phi_x}\hat{\boldsymbol{x}} + p_y e^{j\phi_y}\hat{\boldsymbol{y}})e^{-jkz}$. Then, from (10),

$$\boldsymbol{\mathcal{E}} = p_x\cos(\omega t - kz + \phi_x)\hat{\boldsymbol{x}} + p_y\cos(\omega t - kz + \phi_y)\hat{\boldsymbol{y}} \tag{24}$$

If the x- and y-components are in phase (i.e., $\phi_x = \phi_y$), then (24) can be rewritten as

$$\boldsymbol{\mathcal{E}} = (p_x\hat{\boldsymbol{x}} + p_y\hat{\boldsymbol{y}})\cos(\omega t - kz + \phi_x) \tag{25}$$

and, for any position and time, $\boldsymbol{\mathcal{E}}$ is always parallel to the plane containing $\hat{\boldsymbol{z}}(= \hat{\boldsymbol{k}})$ and $p_x\hat{\boldsymbol{x}} + p_y\hat{\boldsymbol{y}}$. Then, the wave is said to have a *linear polarization*. Note that $\phi_x = \phi_y \pm \pi$ also provides a linear polarization. Now, let us assume that $p_x = p_y = p$ and $\phi_y - \phi_x = \pm\pi/2$. Then, from (24),

$$\boldsymbol{\mathcal{E}} = p[\cos(\omega t - kz + \phi_x)\hat{\boldsymbol{x}} \mp \sin(\omega t - kz + \phi_x)\hat{\boldsymbol{y}}] \tag{26}$$

and the wave has a *circular polarization*, as the tip of $\boldsymbol{\mathcal{E}}$ describes a circular helix in space with an axis in the direction of $\hat{\boldsymbol{z}}$. For $\hat{\boldsymbol{k}} = \hat{\boldsymbol{z}}$, $\phi_y - \phi_x = \pi/2$ ($= -\pi/2$) defines a *left (right) hand circular polarization*. For any other

combination between ϕ_x,ϕ_y and p_x,p_y, the wave polarization is *elliptical*. Finally, from the discussion conducted here, it should be clear that any circular or elliptical polarization can be decomposed into two orthogonal linear polarizations with appropriate amplitude and phase relations. For depictions of different wave polarizations, the reader is referred, for instance, to [19].

3.3 Complex Poynting Vector and Stationary Waves

We will now investigate in further detail the behavior of $\boldsymbol{S}$ for uniform plane waves. From (13) and (21), one verifies that

$$\boldsymbol{S} = \frac{|\boldsymbol{E}|^2}{2\eta}\hat{\boldsymbol{k}} = \frac{\eta|\boldsymbol{H}|^2}{2}\hat{\boldsymbol{k}} \tag{27}$$

indicating that $\boldsymbol{S}$ is real (i.e., a pure active power density) and, consequently, the direction of propagation of a uniform plane wave coincides with the direction of energy flux in a simple medium. For instance, in the examples of Sections 3.1 and 3.2, one immediately observes that $\Re\mathrm{e}(\boldsymbol{S})\|\hat{\boldsymbol{z}}$.

So, let us now extend the example of Section 3.1 to investigate the case of a *stationary wave*, which can be described in terms of two uniform plane waves propagating in opposite directions (i.e., $\hat{\boldsymbol{k}} = \pm\hat{\boldsymbol{z}}$):

$$\begin{aligned}\boldsymbol{E} &= [E_o^+ e^{-jkz} + E_o^- e^{jkz}]\hat{\boldsymbol{x}}\\ \boldsymbol{H} &= (1/\eta)[E_o^+ e^{-jkz} - E_o^- e^{jkz}]\hat{\boldsymbol{y}}\end{aligned} \tag{28}$$

where $\boldsymbol{H}$ was directly obtained from (21), noticing that each individual wave has its $\hat{\boldsymbol{k}}$ pointing in the opposite direction of the other. Substituting (28) into (13), one obtains

$$\boldsymbol{S} = \left[\frac{|E_o^+|^2}{2\eta} - \frac{|E_o^-|^2}{2\eta} + j\frac{|E_o^+||E_o^-|}{\eta}\sin(2kz - \phi^+ + \phi^-)\right]\hat{\boldsymbol{z}} \tag{29}$$

where $\phi^\pm$ are the corresponding phases of $E_o^\pm$. So, (29) indicates that $\boldsymbol{S}$ has real (corresponding to the net flux of power density) and imaginary (corresponding to the stationary reactive power density) parts. This is the case, for instance, of fields on a transmission line terminated by a load that does not match the line impedance. If $|E_o^+| = |E_o^-|$, the wave of (28) is *purely stationary* and there is no average power flux, that is, $\Re\mathrm{e}(\boldsymbol{S}) = \boldsymbol{0}$, which occurs when the line is terminated, for example, by a short circuit.

3.4 Plane Wave Expansion

Due to the linearity of Maxwell's equations, it is possible to show that, by using Fourier transform techniques, an arbitrary solution of Helmholtz equation in free space can be expanded in terms of plane waves in a generic fashion as [18]:

$$\Psi = \int\int_{-\infty}^{\infty} P(k_x, k_y)e^{-j(k_x x + k_y y + k_z z)}dk_x dk_y \tag{30}$$

where $k_z = \pm(k^2 - k_x^2 - k_y^2)^{1/2}$ from (18). Physically, (30) states that an arbitrary wave is in fact a summation of plane waves. Alternatively, from a mathematical point of view (30) represents a double Fourier transform, which may turn into a Fourier series in bounded media problems. $P(k_x, k_y)$ is the representation of the wavefield in the *spectral domain* (or wavenumber domain).

4 WAVES AND SOURCES

Until this point, we have focused our attention on the wave propagation through regions of simple media where no source is present. We shall now present relations describing fields produced by elementary electric current

sources in simple media. The most common way to accomplish this objective is by obtaining the so-called *Green's functions*. For a systematic treatment, the reader is referred to [7] for guided wave examples and [9] for radiation examples with applications to antenna theory. The approach adopted here is more restricted and can be found in most of the suggested bibliography.

Observing from (1) that $\nabla \cdot \boldsymbol{\mathcal{B}} = 0$, one can define the *magnetic vector potential* $\boldsymbol{\mathcal{A}}$ such that $\nabla \times \boldsymbol{\mathcal{A}} = \boldsymbol{\mathcal{B}}$. In simple media, and after applying the *Lorenz gauge condition* given by $c^2 \nabla \cdot \boldsymbol{\mathcal{A}} = -\partial \Phi / \partial t$, where Φ is the *electric scalar potential*, it can be shown that $\boldsymbol{\mathcal{A}}$ satisfies a wave equation as follows [4]:

$$\nabla^2 \boldsymbol{\mathcal{A}} - \frac{1}{c^2} \frac{\partial^2 \boldsymbol{\mathcal{A}}}{\partial t^2} = -\mu \boldsymbol{\mathcal{J}} \tag{31}$$

For time-harmonic fields, this equation can be represented in complex notation as

$$\nabla^2 \boldsymbol{A} + k^2 \boldsymbol{A} = -\mu \boldsymbol{J} \tag{32}$$

A solution of the above can be written in a generic form as [4]

$$\boldsymbol{A} = \mu \int \int \int_V \boldsymbol{J}(\boldsymbol{r}') G(\boldsymbol{r}, \boldsymbol{r}') dv' \tag{33}$$

where V denotes the volumetric region encompassing $\boldsymbol{J}$, $\boldsymbol{r}'$, and $\boldsymbol{r}$ denotes source and observation points, respectively, and $G(\boldsymbol{r}, \boldsymbol{r}')$ is the Green's function. $G(\boldsymbol{r}, \boldsymbol{r}')$ can be interpreted physically as the field produced by a point source, that is, the solution of

$$\nabla^2 G + k^2 G = -\delta(\boldsymbol{r} - \boldsymbol{r}') \tag{34}$$

satisfying the appropriate boundary conditions [4]. For instance, for bounded sources in unbounded simple media (free space), it can be shown that [4]

$$G(\boldsymbol{r}, \boldsymbol{r}') = \frac{e^{-jk|\boldsymbol{r} - \boldsymbol{r}'|}}{4\pi |\boldsymbol{r} - \boldsymbol{r}'|} \tag{35}$$

which is known as the *free-space Green's function*. Furthermore, the time-harmonic electromagnetic field can be written in terms of $\boldsymbol{A}$ as [4]

$$\begin{aligned} \boldsymbol{H} &= \frac{1}{\mu} \nabla \times \boldsymbol{A} \\ \boldsymbol{E} &= -j\omega \left[\boldsymbol{A} + \frac{1}{k^2} \nabla (\nabla \cdot \boldsymbol{A}) \right] \end{aligned} \tag{36}$$

The use of Lorenz gauge condition in the derivation of (31) has an important consequence: one does not need to explicitly consider the charge densities to obtain the field. That should come as no surprise, since charges are related to currents by the continuity equation (3). In the time-harmonic regime their effects become implicit in (36). In any event, it is important to mention that (in a classical sense) gauge conditions other than Lorenz's can be applied [4].

As a simple example, we consider a uniform time-harmonic electric current distribution over a small segment (wire) ℓ along the z-axis, centered at the origin ($z = 0$). The length ℓ is assumed very small, such that $\ell \ll \lambda$. The electric current flows along $\hat{\boldsymbol{z}}$, with a constant phasor I_o for $|z| \leq \ell/2$ ($I_o = 0$ for $|z| > \ell/2$). This source distribution is called *infinitesimal electric dipole*. If the dipole radiates in free space, then the resulting vector potential $\boldsymbol{A}$ is given by (33) and (35). Since $\boldsymbol{r}' = z' \hat{\boldsymbol{z}}$ with $|z'| \leq \ell/2 \ll \lambda$, then $k|\boldsymbol{r} - \boldsymbol{r}'| \approx kr$ and, consequently, $G(\boldsymbol{r}, \boldsymbol{r}') \approx e^{-jkr}/(4\pi r)$. The integral in (33) can then be readily evaluated to give [9]

$$\boldsymbol{A} = \frac{\mu I_o \ell}{4\pi} \frac{e^{-jkr}}{r} \hat{\boldsymbol{z}} \tag{37}$$

where $I_o \ell$ is the *electric dipole moment*. The expressions for the associated electric and magnetic fields are obtained by substituting (37) into (36). The result can be easily extended to arbitrary dipole's locations and orientations [9].

Note from (36) and (37) that the dipole radiation depends on the length ℓ multiplied by k, that is, on the ratio ℓ/λ (also called the *electrical length*). Any bounded source distribution in a simple medium can be written as a superposition of infinitesimal dipoles. As a result, the free-space radiation properties of any bounded source distribution depend on its electrical dimension, that is, its dimension relative to the wavelength. This is also the case for scattering by bounded obstacles immersed in simple media.

We note that the integral (33) is generally difficult to evaluate except for simple current distributions and simple Green's functions, such as the free-space Green's function described in (35).

4.1 Far-Field (Radiation) Region

In free space and for observation points located sufficiently far away from (bounded) sources, (35) and, consequently, (33) can be simplified by means of a Taylor expansion on $|\boldsymbol{r}-\boldsymbol{r}'|$ for small values of $|\boldsymbol{r}'|$ with respect to $|\boldsymbol{r}|$. By keeping just the first few terms on this expansion, one ends up with simplified relations valid for the so-called radiation (or *far-field*) region [9]:

$$\boldsymbol{A} \approx \frac{\mu}{4\pi}\frac{e^{-jkr}}{r}\int\int\int_V \boldsymbol{J}(\boldsymbol{r}')e^{jk\hat{\boldsymbol{r}}\cdot\boldsymbol{r}'}\,dv' \tag{38}$$

where $r = |\boldsymbol{r}|$, in which case relations (36) simplify to

$$\begin{aligned}\boldsymbol{E} &\approx -j\omega[\boldsymbol{A} - (\boldsymbol{A}\cdot\hat{\boldsymbol{r}})\hat{\boldsymbol{r}}]\\ \boldsymbol{H} &\approx (1/\eta)\hat{\boldsymbol{r}}\times\boldsymbol{E}\end{aligned} \tag{39}$$

The above equations imply that $\boldsymbol{E}$ and $\boldsymbol{H}$ are orthogonal to each other, and that both are orthogonal to $\boldsymbol{r}$, which is also the direction of propagation. Hence, the radiation field in the far-field region of a bounded source is a TEM wave.

4.2 Spherical and Cylindrical TEM Wavefronts

A closer look on (38) and (39) reveals some interesting properties of the far-field radiation of bounded sources in simple media. The field dependence on the radial distance r is of the form e^{-jkr}/r. This indicates that the surfaces of constant phase are concentric spheres and that the field intensity decays with $1/r$. Also, the propagation direction (normal to the equiphase surface) is $\hat{\boldsymbol{r}}$. Furthermore, as noted above, $\boldsymbol{E}$, $\boldsymbol{H}$, and $\hat{\boldsymbol{r}}$ are mutually orthogonal. This characterizes a *spherical TEM wave*, for which the basic TEM relations of Section 3 still hold, now with $\hat{\boldsymbol{k}} = \hat{\boldsymbol{r}}$. For instance, a complex E-field notation of the form $\boldsymbol{E} = p(\theta,\phi)(\hat{\boldsymbol{\theta}} \pm j\hat{\boldsymbol{\phi}})e^{-jkr}/r$ characterizes a spherical TEM wave with a circular polarization, according to the basic definitions of Section 3.2. For such wave, the complex Poynting vector is given by $\boldsymbol{S} = \hat{\boldsymbol{k}}|\boldsymbol{E}|^2/(2\eta) = \hat{\boldsymbol{r}}|p(\theta,\phi)|^2/(\eta r^2)$, according to (27).

Such observations show that the average power density of a spherical TEM wave decays with $1/r^2$ in lossless simple media. This result is also expected from simple considerations about energy conservation. Since total radiated power in a lossless medium is conserved and the spherical area of the wavefront increases with r^2, then the power *density* of the spherical wavefront must decay with $1/r^2$. Furthermore, note that a spherical TEM wave behaves *locally* as a plane wave when $kr \gg 1$, so that, in free-space, the field in the vicinity of a receiver antenna located sufficiently far away from the transmitter antenna can be approximated as a plane wave.

Apart from plane and spherical waves, another simple kind of wavefront is the cylindrical one. It is useful to picture a cylindrical wave as the field produced by an infinitely long line current [6]. For observation points far away from the current axis, the corresponding wavefronts can be approximated as cylindrical surfaces with a cross-sectional area that increases linearly with the distance (the cylindrical ρ-coordinate). Consequently, from considerations on energy conservation, the radiating field decays with $\rho^{-1/2}$ [6]. It can also be shown that such

cylindrical wave is also a TEM field obeying those basic relations of Section 3, now with $\hat{\boldsymbol{k}} = \hat{\boldsymbol{\rho}}$. Furthermore, for $k\rho \gg 1$, the cylindrical wavefront can also be *locally* approximated as a plane wave.

More generally, and not just in far-field region, cylindrical and spherical waves are solution of Helmholtz equation (12) in cylindrical and spherical coordinates, respectively. Cylindrical waves are given by [6]:

$$\Psi_{n,k_z} = B_n(k_\rho \rho)h(n\phi)h(k_z z) \tag{40}$$

where $B_n(\cdot)$ is a Bessel function of order n, or combination of them satisfying the boundary conditions, $h(\cdot)$ is an harmonic function, such sine or cosine functions or complex exponentials, and $k_\rho^2 = k^2 - k_z^2$. As linear combinations of functions Ψ_{k_ρ,n,k_z} are also solution of Helmholtz equation, general cylindrical waves can be described as [6]:

$$\Psi = \sum_n \int_{k_z} f(k_z) B_n(k_\rho \rho)h(n\phi)h(k_z z)dk_z \tag{41}$$

where discrete values of n are assumed.

Similarly, solving Helmholtz equation in spherical coordinates results in spherical waves given by [6]:

$$\Psi_{m,n} = b_n(kr)L_n^m(\cos\theta)h(m\phi) \tag{42}$$

where $b_n(\cdot)$ is a spherical Bessel function of order n, related to ordinary Bessel functions by

$$b_n(kr) = \sqrt{\frac{\pi}{2kr}} B_{n+1/2}(kr) \tag{43}$$

and $L_n^m(\cdot)$ are associated Legendre functions. The general solution, assuming discrete values for n and m, is given as [6]:

$$\Psi = \sum_m \sum_n C_{m,n} b_n(kr)L_n^m(\cos\theta)h(m\phi) \tag{44}$$

where $C_{m,n}$ are generic constants (modal coefficients) that depend on the details of the problem.

4.3 Ray Optics Limit

The discussion in the previous section leads toward the picture of TEM wavefronts propagating far away from radiating sources, with directions of propagation normal to the corresponding equiphase surfaces. As stressed previously, distances and dimensions are to be considered large or small vis-a-vis the wavelength of operation. In the limit of $\lambda \to 0$ or, alternatively, $k \to \infty$ the electromagnetic field is expected to locally behave as a TEM wave (i.e., far away from sources). This is often called the *geometrical optics* (GO) limit, where the field propagation can be represented in terms of *rays* with diffraction effects neglected and where a number of other simplifications on the nature of electromagnetic wave propagation can be made [20].

GO principles are directly related to the classical treatment of light. The developments date from Ancient Greece and are intrinsically related to those of Euclidean geometry [2]. Obviously, such studies were not based on Maxwell's equations, but, as expected, the GO principles can be derived from Maxwell's equations. The usual starting point for this derivation is to assume a monochromatic wave (i.e., a time-harmonic field) governed by (12) in complex notation. Adopting the notation of Section 2.1, we let Ψ be a Cartesian component of $\boldsymbol{E}$ or $\boldsymbol{H}$ (a function of position only). Consequently,

$$\nabla^2\Psi + k^2\Psi = 0 \tag{45}$$

From the TEM-waves discussed up to here, it can be assumed, as a first-order *ansatz*, that [2]

$$\Psi \approx p(\boldsymbol{r})e^{-jk_o\Phi(\boldsymbol{r})} \tag{46}$$

where p represents the (complex) amplitude variation, Φ represents the phase variation with position only, and k_o is the wavenumber in vacuum. For other simple media, one can define the *index of refraction*

$$n = \sqrt{(\mu\varepsilon)/(\mu_o\varepsilon_o)} \tag{47}$$

such that $k = nk_o$. In (46), n is accounted for by $\Phi(\boldsymbol{r})$. Furthermore, the wavefront is given by the surfaces of constant $\Phi(\boldsymbol{r})$ (equiphase surfaces). Consequently, the direction of propagation is $\hat{\boldsymbol{k}} = \nabla\Phi/|\nabla\Phi|$. The equation that establishes the optical path (trajectory) in terms of the wavefront properties is accomplished by substituting (46) into (45) and, in the $k_o \to \infty$ limit, assuming that any variation of $p(\boldsymbol{r})$ with position is negligible with respect to that of $k_o\Phi(\boldsymbol{r})$. After some algebraic manipulations, one arrives at the so-called *eikonal equation* [2]:

$$|\nabla\Phi|^2 = n^2 \tag{48}$$

This equation can be used to derive the Fermat's principle below [2]:

$$\Phi(\boldsymbol{r}_2) - \Phi(\boldsymbol{r}_1) = \int_{\boldsymbol{r}_1}^{\boldsymbol{r}_2} n\,d\ell = \int_{t(\boldsymbol{r}_1)}^{t(\boldsymbol{r}_2)} c\,dt \tag{49}$$

where $\Phi(\boldsymbol{r}_2) - \Phi(\boldsymbol{r}_1)$ is the arc length (along the optical path ℓ) between points $\boldsymbol{r}_1$ and $\boldsymbol{r}_2$. This principle states that light (or, more precisely, electromagnetic waves in the GO limit) follows the path corresponding to the shortest travel time [2]. For simple media, both n and c are constants, but (49) holds for inhomogeneous media as well. From (49), one can also derive the laws of reflection and refraction [2] or establish approximate trajectories of radio wave propagation through the atmosphere [21].

GO principles are useful (though approximate) tools for the characterization of electromagnetic wave propagation not only at optical frequencies but also often at RF and microwave frequencies. For instance, such approximation can be used (possibly augmented by small corrections) for characterization of some radio channels at UHF or higher frequencies [22]. The range of validity of such approximation can depend on many factors, but it is fair to say that GO can be used as long as the characteristic lengths of the problem (obstacle feature sizes, mutual distances, medium inhomogeneity scales, etc.) are much larger than λ.

5 WAVES IN LOSSY AND DISPERSIVE MEDIA

So far, we have considered the propagation of electromagnetic waves in simple media without losses or dispersion. This assumption implies that the permittivity and permeability in the constitutive relations (2) and (11) are constant scalar parameters. In general, however, constitutive relations are not that simple. For example, ferroelectric and ferromagnetic materials are examples of *nonlinear media*, where the constitutive parameters at a point depend on the field strength at that point [4]. Even dielectrics can exhibit nonlinear effects under sufficiently large field strengths (e.g., breakdowns inside capacitors or transmission lines). On the other hand, crystals present a well-organized atomic structure, where the field response is highly dependent on the wave polarization. Crystals are examples of *anisotropic* materials, where the permittivity (or permeability) has a tensorial nature [23–26]. The ionosphere is another example of anisotropic medium at radio frequencies, although due to very different reasons [4]. Under certain conditions, the earth subsoil also behaves as an anisotropic medium [27–29].

Wave propagation on nonlinear or anisotropic media will not be considered here. The interested reader may consult Refs. 4 and 23 for more details on that. We shall continue to assume simple (linear, homogeneous, and isotropic) media, but now accounting for the presence of losses (lossy simple media).

In simple media and in the time-harmonic regime, losses in the medium cause a phase delay between the electric displacement $\boldsymbol{D}$ and the electric field $\boldsymbol{\mathcal{E}}$ such that, in complex notation,

$$\boldsymbol{D} = \varepsilon(\omega)\boldsymbol{E} = [\varepsilon'(\omega) - j\varepsilon''(\omega)]\boldsymbol{E} \tag{50}$$

where ε' and $-\varepsilon''$ are the real and imaginary parts of the *complex permittivity* ε, respectively. The negative imaginary part of ε indicates the phase *delay* upon $\boldsymbol{D}$. Here, we still assume that (11) applies for the magnetic relation, since for conductors and dielectrics $\mu \approx \mu_o$ at radio frequencies, although, in general, a complex permeability of the form $\mu(\omega) = \mu'(\omega) - j\mu''(\omega)$ can also be defined [6].

In dielectrics, the ratio $\varepsilon''/\varepsilon'$ defines the *loss tangent*, where $\tan^{-1}(\varepsilon''/\varepsilon')$ is the phase difference between $\boldsymbol{E}$ and $\boldsymbol{D}$ due to the polarization inertia of the atomic structure (macroscopic interpretation). In conductors, net free charges are present and generate a *conduction current* $\boldsymbol{J}_\mathbf{c}$ whenever an external field is applied. For most conductors $\boldsymbol{J}_\mathbf{c}$ is given by Ohm's law [4]

$$\boldsymbol{J}_\mathbf{c} = \sigma \boldsymbol{E} \tag{51}$$

where σ is the material conductivity. In conductive media, $\boldsymbol{J}_\mathbf{c}$ and the corresponding net charge density ρ_c can be subtracted from $\boldsymbol{J}$ and ρ in (9), respectively, and Maxwell's equations in complex notation can be rearranged in the same form of (9), but now with the permittivity replaced by the complex permittivity of (50) with ε' being the real permittivity and $\varepsilon'' = \sigma/\omega$ [6]. After that, $\boldsymbol{J}$ and ρ in (9) correspond to the impressed (external) sources only, as $\boldsymbol{J}_\mathbf{c}$ and ρ_c are implicitly taken into account by the complex ε.

It is important to note that, once the complex permittivity in (50) is adopted, $k = \omega\sqrt{\mu\varepsilon}$ and $\eta = \sqrt{\mu/\varepsilon}$ become complex valued as well. These parameters now depend on ω but are still assumed to be spatially uniform in homogeneous media. Therefore, all the results derived from Maxwell's equations (in complex notation) in previous sections still hold true, except for those where one had to deal with conjugate or absolute values (i.e. relations regarding average energy and power densities). For instance, (4) is still valid, since it is a general definition. However, for a TEM wave propagating in a lossy simple media, (27) must account for the fact that η is now complex valued and hence it generalizes to

$$\boldsymbol{S} = \frac{|\boldsymbol{E}|^2}{2\eta^*}\hat{\boldsymbol{k}} = \frac{\eta|\boldsymbol{H}|^2}{2}\hat{\boldsymbol{k}} \tag{52}$$

5.1 Wave Attenuation and Frequency Dispersion

One of the important consequences of losses is the attenuation of electromagnetic wave inside the medium. To illustrate this, we revisit the problem of Section 3.1, where a uniform plane wave propagates in the $\hat{\boldsymbol{z}}$ direction, but now in a lossy simple medium. From (20), and as the wave is considered uniform, $\boldsymbol{\alpha} \| \boldsymbol{\beta} \| \hat{\boldsymbol{z}}$ and, consequently, $\boldsymbol{k} = k\hat{\boldsymbol{z}} = k\hat{\boldsymbol{k}}$, with k being a complex valued quantity. So, if one defines

$$k = \beta - j\alpha \tag{53}$$

where α and β are nonnegative real quantities, then $\boldsymbol{\alpha} = \alpha\hat{\boldsymbol{k}}$ and $\boldsymbol{\beta} = \beta\hat{\boldsymbol{k}}$. Such definition is valid for any TEM wave propagating through a lossy simple medium in the direction $\hat{\boldsymbol{k}}$. The expressions for α and β are obtained from the definition $k = \omega\sqrt{\mu\varepsilon}$ and (50):

$$\left\{ \begin{array}{c} \alpha \\ \beta \end{array} \right\} = \omega\sqrt{\frac{\mu\varepsilon'}{2}\left(\sqrt{1+\left(\frac{\varepsilon''}{\varepsilon'}\right)^2} \mp 1\right)} \tag{54}$$

The plane wave complex representation of Section 3.1 now becomes

$$\begin{aligned} \boldsymbol{E} &= E_o e^{-\alpha z} e^{-j\beta z}\hat{\boldsymbol{x}} \\ \boldsymbol{H} &= (E_o/\eta) e^{-\alpha z} e^{-j\beta z}\hat{\boldsymbol{y}} \end{aligned} \tag{55}$$

Note again that η is now complex. We observe from (55) that the *phase factor* β controls the phase variation with distance, whereas the *attenuation factor* α controls the amplitude attenuation as the wave propagates (i.e., as z increases). Despite the attenuation effect, the surfaces of constant amplitude and phase are still planes perpendicular to $\hat{\boldsymbol{z}}$, characterizing a uniform plane wave.

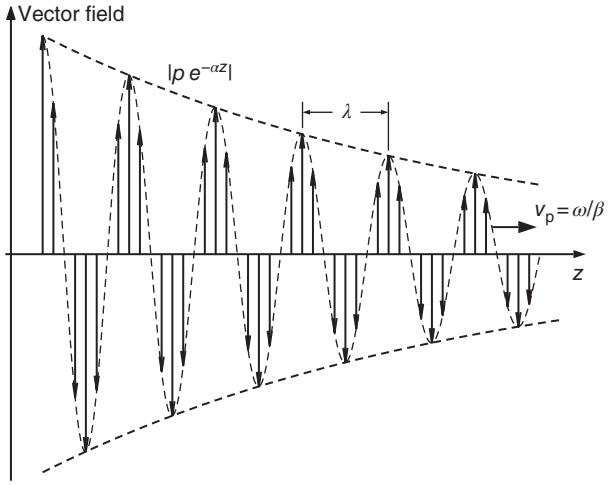

Figure 1 Uniform plane wave propagating in a lossy medium.

Note that the oscillatory behavior is controlled by $e^{-j\beta z}$, and this factor defines the wavelength and phase velocity, now represented as

$$\lambda = 2\pi/\beta \quad \text{and} \quad v_p = \omega/\beta \tag{56}$$

To have a better picture of the wave behavior, we apply the definition in (10) to (55) in order to obtain $\boldsymbol{\mathcal{E}}$ in time domain. Assuming $E_o = pe^{-j\phi}$, then:

$$\boldsymbol{\mathcal{E}} = pe^{-\alpha z}\cos(\omega t - \beta z + \phi)\hat{\boldsymbol{x}} \tag{57}$$

So, the picture here is that of a sinusoidal function (with spatial period λ) multiplied by an envelope variation given by $|pe^{-\alpha z}|$. The field behavior is sketched in Fig. 1 for a fixed instant of time.

By extending the present analysis to the spherical wave solution of Section 4.1, one arrives at a field dependence with the radial distance r according to $e^{-\alpha r}e^{-j\beta r}/r$. The definitions in (56) still apply in this case. Besides the original (algebraic) amplitude attenuation caused by the spherical spreading factor $1/r$, the presence of losses produce an extra attenuation factor $e^{-\alpha r}$.

Equation (54) indicates that both β and α have a nonlinear variation with ω, due to $\varepsilon'(\omega)$ and $\varepsilon''(\omega)$. Consequently, one observes from (56) that v_p varies with ω, that is, different frequency components travel at different phase velocities. This causes the *dispersion* of an electromagnetic signal composed by several frequencies such as a electromagnetic pulse waveform. In RF and microwave applications, electromagnetic waves often comprise a certain frequency bandwidth, and dispersion may cause waveform distortion as the waveform propagates. In general, losses can significantly decrease the signal to noise ratio (SNR) over RF and microwave links and need to be minimized and/or compensated by using, for example, repeaters through long-distance links.

5.2 Group Velocity

As noted above, the phase velocity v_p depends on ω in a dispersive medium. In this case, it becomes necessary to define the velocity of a pulse or wave packet (i.e., a wave composed by different spectral components) since v_p is not unique and no longer adequate. To better understand this aspect, let us consider the simple case of a wave packet composed of two time-harmonic TEM components, propagating in a lossy simple media in the $\hat{\boldsymbol{z}}$ direction and with the same linear polarization, such that

$$\boldsymbol{\mathcal{E}} = [p_1 e^{-\alpha_1 z}\cos(\omega_1 t - \beta_1 z + \phi_1) + p_2 e^{-\alpha_2 z}\cos(\omega_2 t - \beta_2 z + \phi_2)]\hat{\boldsymbol{x}} \tag{58}$$

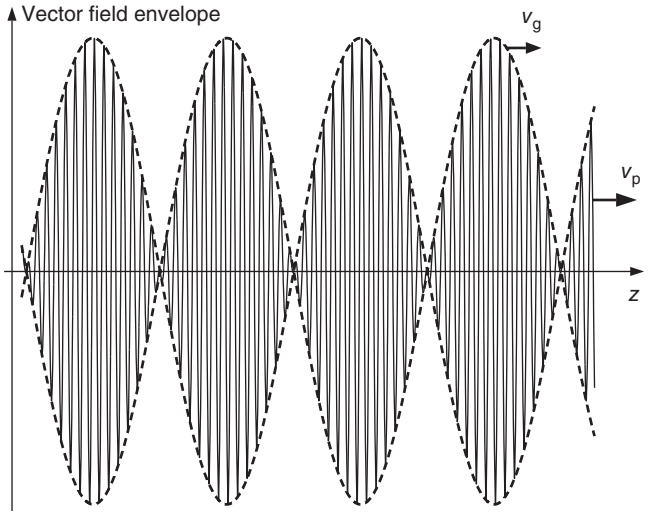

Figure 2 Group and phase velocities for a wave with two spectral components with distinct frequencies.

For the sake of simplicity, we assume $p_1 = p_2 = p$, $\phi_1 = \phi_2 = 0$, and small losses, so that $\alpha_1 \approx \alpha_2 \approx 0$. Furthermore, we define $\omega_c = (\omega_1 + \omega_2)/2$, such that $\omega_{1,2} = \omega_c \mp \delta_\omega$, where $\delta_\omega = (\omega_2 - \omega_1)/2$. By doing so, (58) can be rewritten as

$$\boldsymbol{\mathcal{E}} = 2p\cos[\omega_c t - (\beta_2 + \beta_1)z/2]\cos[\delta_\omega t - (\beta_2 - \beta_1)z/2]\hat{\boldsymbol{x}} \tag{59}$$

which corresponds to the envelope distribution depicted in Fig. 2. The first cosine factor (representing, for instance, a carrier with angular frequency ω_c) propagates with a velocity equal to $2\omega_c/(\beta_2 + \beta_1)$. In the limit $\delta_\omega \to 0$, $(\beta_2 + \beta_1)/2 \approx \beta_c$ (where β_c is the phase constant at ω_c) and, consequently, the carrier's velocity tends to the phase velocity at ω_c. The second cosine factor in (59) modulates the amplitude of the carrier (see Fig. 2) and propagates with a velocity equal to $\delta_\omega/\delta_\beta$, where $\delta_\beta = (\beta_2 - \beta_1)/2$ corresponds to the variation of β around ω_c. We then define the *group velocity*

$$v_g = \lim_{\delta_\omega \to 0} \frac{\delta_\omega}{\delta_\beta} = \left(\frac{\partial \beta}{\partial \omega}\right)^{-1}\Bigg|_{\omega=\omega_c} \tag{60}$$

as the velocity of the wave-packet envelope, which can also be interpreted as the velocity of the signal (information) that modulates the carrier. A spectral analysis will demonstrate that (60) still holds for more arbitrary but band-limited wave packets propagating through a medium with little dispersion (i.e., with relatively small variations of β) [4]. As the wave energy is intrinsically related to the field strength (amplitude), for band-limited signals v_g is also defined as the *velocity of energy flow* [4]. Obviously, $v_g = v_p = c$ for a TEM propagating through a lossless simple media but in general v_p and v_g can be quite different [30, 31]. More detailed discussions on wave velocities can be found in [4] and [5].

6 ELECTROMAGNETIC WAVE INTERACTION WITH OBSTACLES

6.1 Boundary Conditions

Boundary conditions are needed for the proper solution of Maxwell's equations at the interface between two dissimilar media (due to the discontinuity on their physical properties) or at discontinuous source distributions.

One boundary condition is associated to each one of (1) [6]. For a time-invariant interface between two regions 1 and 2, the four boundary conditions read as

$$\begin{aligned} \hat{\boldsymbol{n}} \times (\boldsymbol{\mathcal{E}}_2 - \boldsymbol{\mathcal{E}}_1) &= 0 \qquad & \hat{\boldsymbol{n}} \cdot (\boldsymbol{\mathcal{D}}_2 - \boldsymbol{\mathcal{D}}_1) &= q_s \\ \hat{\boldsymbol{n}} \times (\boldsymbol{\mathcal{H}}_2 - \boldsymbol{\mathcal{H}}_1) &= \boldsymbol{\mathcal{J}}_s \qquad & \hat{\boldsymbol{n}} \cdot (\boldsymbol{\mathcal{B}}_2 - \boldsymbol{\mathcal{B}}_1) &= 0 \end{aligned} \tag{61}$$

where $\hat{\boldsymbol{n}}$ is the unit normal to the interface pointing from region 1 toward region 2, and $\boldsymbol{\mathcal{J}}_s$ and q_s denote surface (or line) current and charge distributions over the interface, respectively. In (61), the field components are evaluated right next to each side of the interface, at region 1 or 2, respectively. In the time-harmonic regime, the complex representation of the boundary conditions have the same form as (61). If both regions represent simple media, then (11), (50), and the complex representation of (61) gives

$$\begin{aligned} \hat{\boldsymbol{n}} \times (\boldsymbol{E}_2 - \boldsymbol{E}_1) &= 0 \qquad & \hat{\boldsymbol{n}} \cdot (\varepsilon_2 \boldsymbol{E}_2 - \varepsilon_1 \boldsymbol{E}_1) &= \rho_s \\ \hat{\boldsymbol{n}} \times (\boldsymbol{H}_2 - \boldsymbol{H}_1) &= \boldsymbol{J}_s \qquad & \hat{\boldsymbol{n}} \cdot (\mu_1 \boldsymbol{H}_2 - \mu_1 \boldsymbol{H}_1) &= 0 \end{aligned} \tag{62}$$

where μ_i and ε_i refer to region i ($i = 1, 2$).

In simple media and if no surface currents or charges are present at the interface, both (61) and (62) indicate that the tangential (to the interface) components of the electric and magnetic fields must be continuous across the interface. These are the only boundary conditions that must be imposed for the proper wave solution as at regions of a simple medium without sources only Faraday's and Ampère's laws are needed [6]. A particular case of interest is that at the interface of a perfect electric conductor, which will be discussed in Section 6.3.

6.2 Reflection and Refraction of Plane Waves

Plane wave reflection and refraction at a planar interface is a canonical problem in electromagnetic wave theory and provides many useful insights about the behavior of waves in the presence of more general obstacles [32–35]. Consider a plane interface between two simple media (lossy or not), characterized by their (complex) permeabilities (μ_1 and μ_2) and permittivities (ε_1 and ε_2), as shown in Fig. 3. An incident plane wave (index i) impinges upon the interface from medium 1, generating a reflected plane wave (index r), propagating back into medium 1, and a transmitted plane wave (index t) into medium 2. The exact reflected and transmitted energies of the corresponding waves depend on the media properties and on the direction of propagation and polarization of the incident wave.

Any arbitrary polarization can be decomposed into two linear and orthogonal ones in simple media (see Section 3.2). For the present analysis, the commonly used are the perpendicular (no E-field component normal to the interface) and parallel (no H-field component normal to the interface) linear polarizations, as depicted in Fig. 3a and Fig. 3b, respectively. The formulas to be presented are valid for any incident plane wave, being it

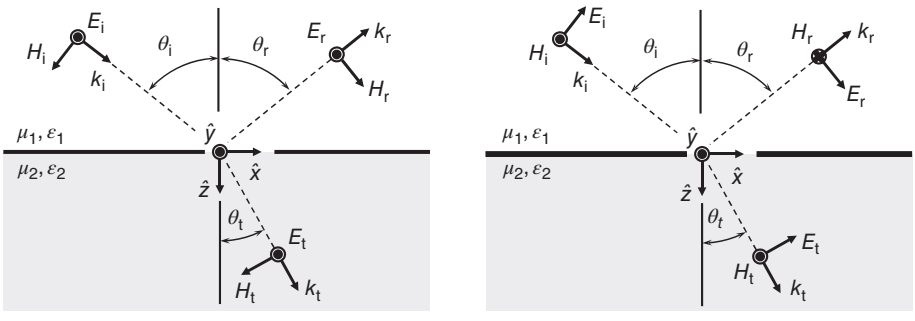

Figure 3 Plane wave incidence upon a plane interface: (a) perpendicular and (b) parallel polarizations.

uniform or not. According to the discussion in Section 3, the geometrical interpretation illustrated in Fig. 3 (i.e., with real-valued θ angles) is valid only for uniform waves. Depending on the case, some θ angles may come out complex, indicating that the corresponding plane wave is nonuniform. In any event, Fig. 3 is indeed useful to establish the tangential (and normal) components of the fields at the interface, necessary for the application of the pertinent boundary conditions and, consequently, the solution of the problem. For uniform waves, Fig. 3 also provides a nice picture of the problem.

We will assume a time-harmonic regime (i.e., monochromatic waves) and use the complex phasor notation. According to (19), we can assume, without loss of generality, that the incident propagation vector ($\boldsymbol{k}_\mathbf{i}$) has no component in the $\hat{\boldsymbol{y}}$ direction. The boundary conditions will further yield that the same is true for the reflected ($\boldsymbol{k}_\mathbf{r}$) and transmitted ($\boldsymbol{k}_\mathbf{t}$) propagation vectors. With that in mind, we can define the xz-plane in Fig. 3 as the *plane of incidence*. For uniform plane waves, that is in conformity with Fermat's principle: the trajectories are rectilinear (in simple media) and corresponding to the least travel time (see Section 4.3).

Starting with the perpendicular polarization and with the help of (17) and Fig. 3a, we define the electric fields of the plane waves as

$$\begin{aligned}\boldsymbol{E}_\mathbf{i} &= E_o e^{-j\boldsymbol{k}_\mathbf{i}\cdot\boldsymbol{r}}\hat{\boldsymbol{y}}\\ \boldsymbol{E}_\mathbf{r} &= \Gamma_\perp E_o e^{-j\boldsymbol{k}_\mathbf{r}\cdot\boldsymbol{r}}\hat{\boldsymbol{y}}\\ \boldsymbol{E}_\mathbf{t} &= T_\perp E_o e^{-j\boldsymbol{k}_\mathbf{t}\cdot\boldsymbol{r}}\hat{\boldsymbol{y}}\end{aligned} \tag{63}$$

where $\Gamma_\perp$ and $T_\perp$ are the Fresnel's reflection and transmission coefficients for the perpendicular polarization, respectively, relating the amplitude and phase of the corresponding field to those of the incident one. The propagation vectors are written as

$$\begin{aligned}\boldsymbol{k}_\mathbf{i} &= k_1(\sin\theta_\mathrm{i}\hat{\boldsymbol{x}} + \cos\theta_\mathrm{i}\hat{\boldsymbol{z}})\\ \boldsymbol{k}_\mathbf{r} &= k_1(\sin\theta_\mathrm{r}\hat{\boldsymbol{x}} - \cos\theta_\mathrm{r}\hat{\boldsymbol{z}})\\ \boldsymbol{k}_\mathbf{t} &= k_2(\sin\theta_\mathrm{t}\hat{\boldsymbol{x}} + \cos\theta_\mathrm{t}\hat{\boldsymbol{z}})\end{aligned} \tag{64}$$

where $k_j = \omega\sqrt{\mu_j\epsilon_j}$ (with $j = 1, 2$). Note that (64) is in agreement with (18). From (19), (63), and (64), one immediately obtains the H-field expressions, observing that $\eta = \eta_j = \sqrt{\mu_j/\epsilon_j}$, with $j = 1$ for the incident and reflected waves and $= 2$ for the transmitted wave.

Enforcing the boundary conditions (i.e., the continuity of the tangential E- and H-field components) at the interface plane $z = 0$, one obtains the *Snell's law*

$$k_1\sin\theta_\mathrm{i} = k_1\sin\theta_\mathrm{r} = k_2\sin\theta_\mathrm{t} \tag{65}$$

and also with

$$\begin{aligned}\Gamma_\perp &= \frac{\eta_2\cos\theta_\mathrm{i} - \eta_1\cos\theta_\mathrm{t}}{\eta_2\cos\theta_\mathrm{i} + \eta_1\cos\theta_\mathrm{t}}\\ T_\perp &= \frac{2\eta_2\cos\theta_\mathrm{i}}{\eta_2\cos\theta_\mathrm{i} + \eta_1\cos\theta_\mathrm{t}}\end{aligned} \tag{66}$$

The Snell's law (65) is a simple consequence of the matching of the phase variation of the fields at the interface, a requirement for field continuity. For a uniform incident wave (with a real-valued θ_i), (65) imposes that $\theta_\mathrm{r} = \theta_\mathrm{i}$ (i.e., the reflected wave is also uniform), which is the law of reflection known for centuries in optics and in conformity with Fermat's principle [2]. The Snell's law for refraction is given by the second equality in (65), which can be rewritten with the help of (47):

$$n_1\sin\theta_\mathrm{i} = n_2\sin\theta_\mathrm{t} \tag{67}$$

where $n_{1,2}$ are the indices of refraction at regions 1 and 2, respectively. Equations (65) and (67) provide the value of θ_t with respect to θ_i and the physical properties of the media. Again, the presence of a complex valued θ_t just

indicates that the transmitted wave is nonuniform. That may happen even for a uniform incident wave if losses are present in one of the media (resulting in a complex index of refraction) or under conditions of *total reflection* (see below).

The analysis of the parallel polarization follows along a similar line to that of its perpendicular counterpart and a comparison between Figs. 3a and 3b provides the necessary insights. After the enforcement of the boundary conditions at the interface, one comes up with (65) and (67) once more (i.e., Snell's law is valid for any polarization) and

$$\Gamma_{\parallel} = \frac{\eta_2 \cos\theta_t - \eta_1 \cos\theta_i}{\eta_2 \cos\theta_t + \eta_1 \cos\theta_i}$$
$$T_{\parallel} = \frac{2\eta_2 \cos\theta_i}{\eta_2 \cos\theta_t + \eta_1 \cos\theta_i} \tag{68}$$

which are the Fresnel's reflection and transmission coefficients for the parallel polarization, respectively.

For simplicity, we shall assume next that both media are lossless simple dielectrics (i.e., $\mu_1 \approx \mu_2 \approx \mu_o$ and real-valued ε_1 and ε_2) and that the incident plane wave is uniform (θ_i is real). The incidence is defined *external* if $\varepsilon_2 > \varepsilon_1$ (for instance, the incidence of a radio wave upon ground in a RF link). For real-valued θ_t, (67) provides that $\theta_t < \theta_i$ for external incidences. Otherwise, the incidence is *internal* (e.g., a refraction from water into air).

The behavior of $|\Gamma|$ and $|T|$ with respect to θ_i is sketched in Figs. 4a and 4b for external and internal incidence, respectively. From the figures, one observes two particular angles of incidence: the *Brewster* (or polarizing) angle θ_B, for which $|\Gamma_{\parallel}| = 0$, and the *critical* angle θ_C, such that, at internal incidence and for $\theta_i \geq \theta_C$, $|\Gamma| = 1$ and *total reflection* occurs. For lossless and simple media, the Brewster angle only occurs for parallel polarization [2]. Its value can be determined from (67) and (68) by setting $\Gamma_{\parallel} = 0$:

$$\tan\theta_B = n_2/n_1 \tag{69}$$

If losses are present, then $\Gamma_{\parallel}$ is complex and $|\Gamma_{\parallel}| = 0$ is never met for any θ_i. Instead, $|\Gamma_{\parallel}|$ passes through a minimum and that defines an *effective* Brewster angle. In any event, one can infer from Fig. 4 that $|\Gamma_{\parallel}| < |\Gamma_{\perp}|$ for $0 < \theta_i < \pi/2$. For this reason, polarizing glasses are designed to block horizontally polarized light reflected by the ground. For this reason also, vertically polarized RF waves are preferred when attempting to obtain a uniform coverage of a urban cell in mobile communications at UHF (due to reflections from vertical buildings) [36].

In lossless simple media, the critical angle θ_C occurs just at internal incidence. This is established from (67) and from the fact that $n_1 > n_2$ for internal incidence, yielding $\theta_t > \theta_i$ for $\theta_i \leq \theta_C$ with $\theta_t = \pi/2$ when $\theta_i = \theta_C$ by

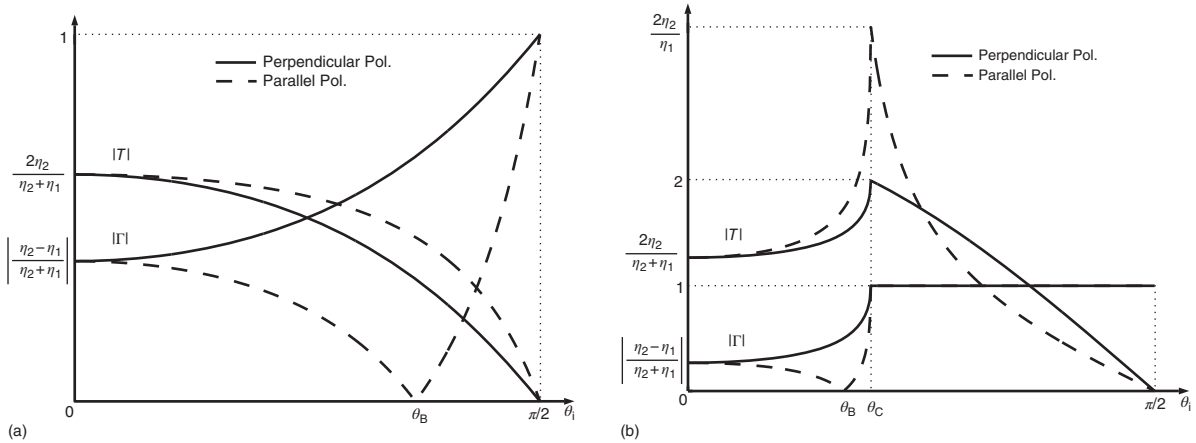

Figure 4 $\|\Gamma\|$ and $\|T\|$ as a function of θ_i: (a) external and (b) internal incidences.

definition. Besides, θ_t becomes complex for $\theta_C < \theta_i \leq \pi/2$, indicating that the transmitted wave is nonuniform for incidence angles greater than θ_C. The primary consequence is $|\Gamma| = 1$ for $\theta_i \geq \theta_C$, as depicted in Fig. 4b.

To better understand the behavior of the transmitted wave at total reflection, let us recall the propagation vector $\boldsymbol{k_t}$ of (64). For the present scenario and from (65), one will verify that the x-component of $\boldsymbol{k_t}$ is real valued while its z-component is purely imaginary, such that the transmitted wave propagates along the $\hat{\boldsymbol{x}}$ direction while its intensity dies off exponentially from the interface. So, the transmitted wave is strongly localized nearby the interface and propagates parallel to it, characterizing a *surface wave*. Also, if one obtains the $\boldsymbol{E}$ and $\boldsymbol{H}$ field components—with the help of (21) and (64)—and substitutes them into (13), it will be shown that the complex Poynting vector has a purely imaginary $\hat{\boldsymbol{z}}$ component and, consequently, there is no average flux of active (real) power through the interface (i.e., the incident power is totally reflected by the interface). In practical situations, losses will prevent such idealized conditions from happening and a (small) amount of energy will be eventually transmitted through the interface [4]. The critical angle and the consequent total reflection help in providing a nice picture on how light is guided throughout an optical fiber [37].

6.3 Waves upon Good Electric Conductors

The equations of Section 6.2 can also be used to investigate the behavior of a plane wave incidence upon the surface of a good electric conductor. Let us assume in Fig. 3 that region 1 is a lossless simple media (i.e., μ_1 and ε_1 are real valued constants), while region 2 is a good conductor, in which case, $\mu_2 \approx \mu_o$ and ε_2 is complex and in according to (50). By definition, for good conductors $\sigma \gg \omega\varepsilon$, such that $\varepsilon_2 \approx -j\sigma/\omega$ for our purposes, where σ is the conductivity of region 2. Consequently, $k_2 \approx \sqrt{-j\omega\mu_o\sigma}$ and $\eta_2 \approx \sqrt{j\omega\mu_o/\sigma}$.

Applying such definitions to (65), one should observe that $\theta_i = \theta_r$, as expected, and that $\theta_t \approx \pi/2$ as $\sigma \to \infty$. Besides, from (64), it is verified that $\boldsymbol{k_t} \approx k_2\hat{\boldsymbol{z}} \approx \sqrt{-j\omega\mu_o\sigma}\hat{\boldsymbol{z}}$. So, we come to the conclusion that the transmitted plane wave tends to behave as a uniform one inside the good conductor, propagating in the direction normal to the conductor's surface. The corresponding amplitude factor $\alpha_2 \approx \sqrt{(\omega\mu_o\sigma)/2}$ has a considerably large value, so that the field intensity dies off very rapidly away from the surface (tending to zero when $\sigma \to \infty$, as expected). Thus, a *skin depth* δ is defined as the propagation distance needed for the field intensity to decay by a factor $1/e$, that is, $\delta = 1/\alpha_2 \approx \sqrt{2/(\omega\mu_o\sigma)}$.

As a consequence, $\boldsymbol{E_t}$ is highly concentrated nearby and parallel to the surface. So, from (51), we end up concluding that there will be a volumetric conduction current highly concentrated nearby and flowing parallel to the conductor's surface. In the limit of a perfect electric conductor (i.e., $\sigma \to \infty$), such current behaves as a surface one ($\boldsymbol{J_s}$), in which case, (61) and (62) apply with null fields inside region 2 (note that $\hat{\boldsymbol{n}} = \hat{\boldsymbol{z}}$ in Fig. 3).

It is interesting to stress that the results presented here are valid for any angle of incidence θ_i and for any wave polarization. So, according to the discussion in the beginning of Section 3, the results are valid for any electromagnetic wave impinging upon the planar surface of a good electric conductor.

The limiting case of a perfect electric conductor is not useful just for good conductors. As an example, let us assume an horizontally polarized radio wave propagating over ground and at *grazing incidence* (i.e., with $\theta_i \to \pi/2$, which is generally the case in a long-distance UHF radio link). This corresponds to a perpendicular polarization and, according to (66), $\Gamma_\perp \to -1$. Note also from (66) that $\Gamma_\perp \to -1$ as well for incidences upon a good electric conductor, as $|\eta_2| \to 0$ in this case. So, it is often used to approximate the ground as a perfect (or good) electric conductor to simplify the analysis [21]. For vertical polarization the approximation to be adopted also depends on other factors (like the value of θ_B) [21].

6.4 Scattering and Diffraction

The scattering of an electromagnetic wave by an arbitrary obstacle is in general a difficult problem to solve using purely analytical techniques. Usually, numerical methods based on different discretization techniques [38] may

be employed. Among these, one can cite the method of moments [39, 40], the finite-element method [41], and the finite-difference time-domain method [15]. However, if the incident wave is locally TEM and if the obstacle is immersed in a simple media and has a smooth surface, the concepts discussed in Sections 4.3 and 6.2 can be adopted (as approximations) as long as the obstacle's dimensions are large compared to the wavelength. Corrections to account for the curvatures of the incident wavefront (in case it is not a plane wave) and of the obstacle surface can be derived from GO principles and included in Γ of (66) and (68), according to the wave polarization [20, 42]. The procedure is then conducted by *tracing rays* from the transmitter point to the receiver, such that any reflection upon the obstacle must obey Fermat's principle, that is, the trajectories are rectilinear (in simple media) and $\theta_i = \theta_r$ with respect to the surface's normal. The difficulty of such technique generally appears in the determination of the *specular* points (where reflection occurs) over the surface of the obstacle.

If the obstacle presents curvature discontinuities (e.g., at the edge of a wedge or at the border of a reflector antenna), then the propagation mechanisms associated to the incidence upon such regions is classified as a *diffraction* (as the diffraction of a laser beam by a metallic slit). Asymptotic techniques (in the sense of being applicable in the limit of very large wavenumber k) based on the geometrical theory of diffraction (GTD) or the uniform theory of diffraction (UTD) can be applied to account for diffraction [42, 43]. Such techniques are also based on ray tracing and can be accommodated together with GO principles to characterize the wave propagation through regions with several obstacles, like a urban scenario in mobile communications [22, 44].

7 GUIDED WAVES

Electromagnetic waves can propagate either in open space or through guiding structures such as transmission lines and waveguides. The choice of transmission lines depend on characteristics such as frequency of operation, bandwidth, power handling capability, and losses. Some of the most usual transmission lines are two-wire lines, coaxial cables, rectangular and circular waveguides, microstrips, optical fibers, and striplines. These structures are discussed in more detail in [45].

Some authors employ the *waveguide* denomination for guiding structures that allow propagation only of *transverse electric* (TE) and/or *transverse magnetic* (TM) waves, as described below, while the term *transmission lines* is used for guiding structures that allow propagation of TEM waves as well. Other authors use these terms interchangeably, as we will do here. We discuss TE and TM waves next.

7.1 TE and TM Waves

We will assume that the waves are guided in z-direction. TE and TM waves are a class of solutions for Maxwell's equations. As we are looking for propagating fields, their z-dependence will be assumed on the form $e^{-jk_z z}$. In this case, the transverse components of the electric and magnetic fields can be written as [33]:

$$\begin{aligned}\boldsymbol{E}_\mathbf{t} &= \frac{1}{k^2 - k_z^2}\left[-j\omega\mu\left(\nabla_\mathrm{t} H_z\right)\times\hat{\boldsymbol{z}} - jk_z\nabla_\mathrm{t} E_z\right]\\ \boldsymbol{H}_\mathbf{t} &= \frac{1}{k^2 - k_z^2}\left[j\omega\varepsilon\left(\nabla_\mathrm{t} E_z\right)\times\hat{\boldsymbol{z}} - jk_z\nabla_\mathrm{t} H_z\right]\end{aligned} \tag{70}$$

where ∇_t stands for the transverse portion of the ∇ operator. The electric field of the TE component is entirely transverse ($E_z = 0$), while the magnetic field has a longitudinal component ($H_z \neq 0$). From (70), the TE field is generated from the longitudinal magnetic field H_z, and the corresponding transverse components $\boldsymbol{E}_\mathbf{t}$ and $\boldsymbol{H}_\mathbf{t}$. On the other hand, the magnetic field of the TM component is entirely transverse ($H_z = 0$), while the electric field has a longitudinal component ($E_z \neq 0$). From (70), the TM field is given by the longitudinal electric field E_z, and the corresponding transverse components.

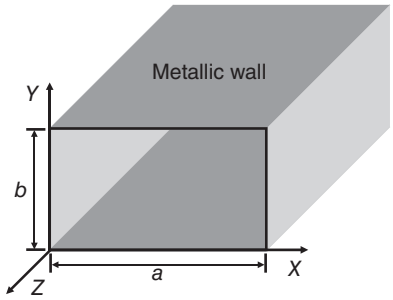

Figure 5 Rectangular waveguide geometry.

TE and TM waves are supported by waveguides containing one or more perfect conductors and a homogeneous dielectric. In this case, each wave (or mode) satisfies the boundary conditions at the waveguide walls and are decoupled from each other. A useful example of such structure is the rectangular waveguide, formed by four metallic walls (perfect conductors), as shown in Fig. 5. In general, a rectangular waveguide may be empty inside or *loaded*, that is, partially or completely filled with a dielectric. We will consider homogeneous (i.e., empty or completely filled with a uniform dielectric) rectangular waveguides next.

For TE modes (also known as H modes), the longitudinal component of the magnetic field, $H_z(x, y, z)$ is given by the solution of the scalar wave equation that satisfies the appropriate boundary conditions at the four metallic walls (in this case, $\partial H_z/\partial n = 0$), that is:

$$H_z = H_o \cos\left(\frac{m\pi x}{a}\right) \cos\left(\frac{n\pi y}{b}\right) e^{-jk_z z} \tag{71}$$

where $k_z = \sqrt{k^2 - (m\pi/a)^2 - (n\pi/b)^2}$, m integer ≥ 0, n integer ≥ 0 (but not $m = n = 0$). The transverse components of the electric and magnetic fields can be obtained directly from (70). These modes are called TE_{mn}, in reference to the indexes m and n of (71). According to the frequency of operation, the TE_{mn} modes may propagate or not inside the waveguide. A propagating mode is characterized by a real k_z. The parameter k_z is real only if $k^2 > (m\pi/a)^2 + (n\pi/b)^2$. Otherwise, the mode is evanescent (exponentially decaying). The threshold frequency is called *cutoff frequency* and is given by

$$f_{mn} = \frac{1}{2\sqrt{\mu\epsilon}} \sqrt{\left(\frac{m}{a}\right)^2 + \left(\frac{n}{b}\right)^2} \tag{72}$$

For TM modes (also known as E modes), the longitudinal component of the electric field is obtained from the solution of the scalar wave equation satisfying the boundary conditions at the four metallic walls (in this case, $E_z = 0$), that is:

$$E_z = E_o \sin\left(\frac{m\pi x}{a}\right) \sin\left(\frac{n\pi y}{b}\right) e^{-jk_z z} \tag{73}$$

where m integer > 0, n integer > 0, and k_z is the same as above. The transverse components of the fields are obtained substituting (73) into (70). Again the TM_{mn} modes only propagate for frequencies above the cutoff frequency f_{mn} given by (72).

Assuming that $a > b$, the first mode that propagates (i.e., smallest cutoff frequency) is the TE_{10}, which is called *dominant mode*. Usually, waveguides are designed to operate in a frequency range where only the dominant mode can propagate. This avoids inter-modal dispersion that results from the different phase velocities of two or more propagating modes. Note that if the waveguide is filled with a lossy dielectric, the modes are attenuated even above cutoff. Mathematically, TE and TM modes are orthogonal to each other and form a complete set. This means that any field distribution inside the waveguide can be represented as a superposition of TE and TM modes [7]. However, when the finite conductivity of the metallic walls are considered, this orthogonality is no longer valid, and the modes become coupled. Also, when the dielectric is not homogeneous, the propagating modes become a combination of TE and TM fields, also called *hybrid modes* [7].

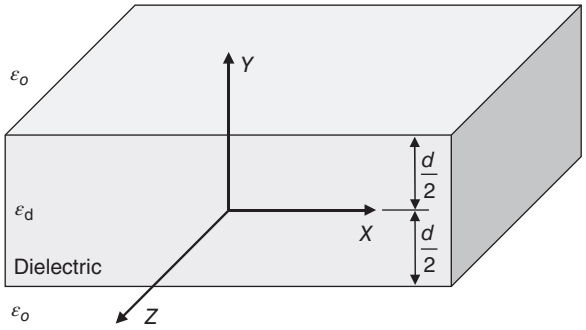

Figure 6 Dielectric slab waveguide.

7.2 Surface and Leaky Waves

Surface waves were introduced in Section 6.2, under the condition of total internal reflection. This type of wave exhibits an exponential decay away from a guiding interface, while propagating in a direction parallel to it. Such wave is also supported by dielectric waveguides, where no conductor is used to guide the fields. A simple example of this kind of waveguide is the dielectric slab waveguide, formed by a dielectric layer (infinite in $\hat{\boldsymbol{x}}$ direction), surrounded by air, as shown in Fig. 6. In the air, surface wave modes are evanescent, and there is no average power flow from the dielectric to the air. TE and TM modes can be obtained for dielectric waveguide by following a procedure similar to the one described in Section 6.1 [6]. For TE and TM modes, there is also a possibility of even and odd modes. For example, even TM modes are given by [6]:

$$E_z = \begin{cases} E_d \cos(\beta_y y) e^{-jk_z z}, & \text{for } |y| \le d/2 \\ E_o e^{-\alpha_y |y|} e^{-jk_z z}, & \text{for } |y| \ge d/2 \end{cases} \tag{74}$$

The associated transverse field components are obtained by substituting (74) into (70). The characteristic equations in the dielectric and in the air are given by $k_z^2 + \beta_y^2 = \omega^2 \mu_o \varepsilon_d$ and $k_z^2 - \alpha_y^2 = \omega^2 \mu_o \varepsilon_o$. The boundary conditions at the dielectric interfaces provide the relation between the amplitudes $[E_d \cos(\beta_y d/2) = E_o e^{-\alpha_y d/2}]$ and require that

$$\beta_y \cot(\beta_y d/2) = -\alpha_y \varepsilon_d / \varepsilon_o \tag{75}$$

which is the transcendental equation for k_z and, consequently, β_y and α_y. Multiple solutions of this transcendental equation are often identified by a subscript n (TM_n mode).

These modes present surface waves properties when α_y is real and positive. The cutoff frequency of the TM_n mode is the lowest frequency for which it propagates with no attenuation $[\alpha_y = 0,\ \beta_y = \omega\sqrt{\mu_o(\varepsilon_d - \varepsilon_o)}]$. In this case, (75) results in

$$f_n = \frac{n}{2d\sqrt{\mu_o(\varepsilon_d - \varepsilon_o)}}, \text{ with } n = 1, 3, 5, \ldots \tag{76}$$

For frequencies below the cutoff, the power is no longer confined within the dielectric, and part of it is radiated into air. As a consequence of this radiation loss, the modes propagate with attenuation, having complex $k_z = \beta_z - j\alpha_z$. This kind of wave is called a *leaky wave*. A simple interpretation of these waves comes from the plane wave expansion of a field within the dielectric. As mentioned earlier, any field can be written as a superposition of plane waves in a sourceless linear medium. From the dielectric interface problem, it is known that plane waves with incidence angles above critical angle will be totally reflected back to the dielectric, forming a surface wave. But those plane waves with incidence angles below critical angle will be refracted into air (radiation), forming a leaky wave. Odd TM modes and both even and odd TE modes can be obtained similarly and present the same properties as described for even TM modes [6].

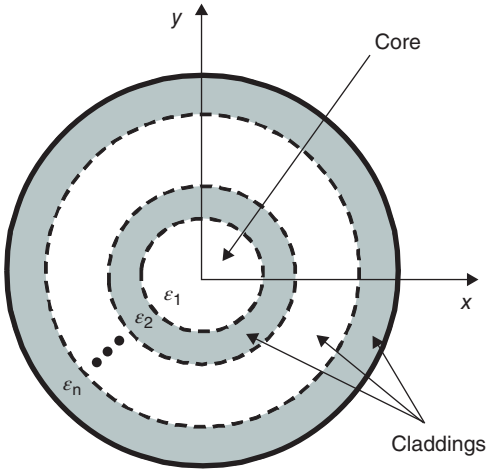

Figure 7 Cross-section of an optical fiber.

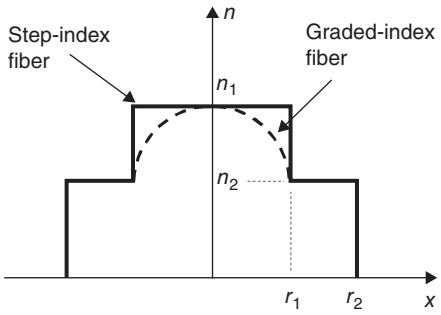

Figure 8 Profiles of optical fibers: step-index and graded-index fibers.

An important example of dielectric waveguide is the optical fiber [37, 46], which is extensively used in long-distance and high-bandwidth communications. It is often used in communication systems with wavelengths ranging from 800 nm to 2.55 μm, near visible spectrum. An optical fiber is formed by a dielectric rod, called *core*, and one or more surrounding cylindrical dielectric layers, called *claddings*. A cross-section of an optical fiber is shown in Fig. 7.

In the simplest format, only one cladding is used. Usually, the refraction index of the core is slightly above that of the cladding, allowing the propagation of surface waves. When the refraction index of the core is constant, the configuration is known as a step-index fiber. Otherwise, it is known as a graded-index fiber, as shown in Fig. 8, where r_1 and r_2 are the radius limits of the core and cladding, respectively.

A very simple explanation for propagation within step-index optical fibers can be obtained using ray optics, as shown in Fig. 9. The refraction index of the core (n_1) is larger than that of the cladding (n_2), and the waves in the core are totally reflected at the core–cladding interface, as long as the incidence angles (θ_{in}) are larger than the critical one (θ_c).

Similar to the dielectric slab waveguide, there are fields in the cladding, but they present an evanescent behavior and do not carry power away from the core. On the other hand, for an optical fiber, pure TE modes or TM modes are only allowed when there is no azimuthal variation. In general, the presence of both longitudinal components is required in order to satisfy the boundary conditions (62) at the core–cladding interface, resulting in hybrid modes. As explained earlier, E_z and H_z are solution of the wave equation in cylindrical coordinates (40). In the core ($r < r_1$), they can be written as [46]:

$$E_z^< = a_\nu^< J_\nu(u\rho)e^{j\nu\phi}e^{-j\beta z}$$

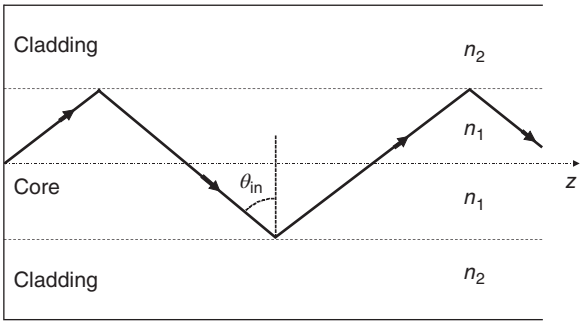

Figure 9 Ray optics applied to a step-index optical fiber.

$$H_z^< = b_\nu^< J_\nu(u\rho)e^{j\nu\phi}e^{-j\beta z} \tag{77}$$

where $J_\nu(\cdot)$ is the Bessel function of first kind of order ν ($\nu = 0, 1, 2, \ldots$), which satisfies the finite condition at $\rho = 0$, and

$$u^2 = k_1^2 - \beta^2 \tag{78}$$

where k_1 is the wavenumber at the core.

Similarly in the cladding ($r > r_1$), E_z and H_z can be written as [46]:

$$\begin{aligned} E_z^> &= a_\nu^> K_\nu(t\rho)e^{j\nu\phi}e^{-j\beta z} \\ H_z^> &= b_\nu^> K_\nu(t\rho)e^{j\nu\phi}e^{-j\beta z} \end{aligned} \tag{79}$$

where $K_\nu(\cdot)$ is the modified Bessel function of the second kind of order ν ($\nu = 0, 1, 2, \ldots$), which satisfies the radiation condition as $\rho \to \infty$, and

$$t^2 = \beta^2 - k_2^2 \tag{80}$$

where k_2 is the wavenumber at the cladding. In both regions, the transverse components of the electric and magnetic fields are obtained using (70). The fields in both regions have the same variation in the z-direction ($e^{-j\beta z}$), as required for phase matching at the interface. Imposing the boundary conditions (62) results in the transcendental equation for the hybrid modes [46]:

$$\left[\frac{J'_\nu(ua)}{uJ_\nu(ua)} + \frac{K'_\nu(ta)}{tK_\nu(ta)}\right]\left[k_1^2\frac{J'_\nu(ua)}{uJ_\nu(ua)} + k_2^2\frac{K'_\nu(ta)}{tK_\nu(ta)}\right] = \left(\frac{\beta\nu}{a}\right)^2\left(\frac{1}{u^2} + \frac{1}{t^2}\right)^2 \tag{81}$$

Numerical solutions of (81), together with (78) and (80), lead to the values of phase constants of the propagating modes, at the given frequency and for an azimuthal number ν. The dominant mode, that propagates for any frequency, is called HE_{11}, which comes from the first solution of (81) for $\nu = 1$.

An important parameter of an optical fiber is the *V parameter* (or *V number*):

$$V = \left(\frac{2\pi a}{\lambda}\right)^2 (n_1^2 - n_2^2) \tag{82}$$

The V parameter determines the number of modes that propagate in the fiber. If $V \leq 2.405$, only the dominant HE_{11} mode propagates. Very small core radius leads to very high cut-off frequency of first higher order modes, which explains their high bandwidths. Optical fibers that allow only one mode to propagate are called single-mode, otherwise they are called multimode fibers. Usually, the latter has larger core radius, which make it easier to couple the light from optical sources, like light-emitting diodes (LEDs). On the other hand, multimode fibers present intermodal dispersion, which can limit their use.

In the above, we discussed the analytical treatment of waveguides with canonical geometries and assumed no geometry variations along the direction of propagation. For the analysis of waveguides with complex geometries

that may include general discontinuities and/or curved or tapered sections, it become necessary to employ numerical methods of analysis [47] or semi-analytical methods based on mode matching [48, 49] or perturbation techniques [50].

8 COHERENT AND NONCOHERENT WAVES

Electromagnetic waves can also be classified as coherent or noncoherent [2]. Coherent waves have definite phase fronts (for each wavelength), while noncoherent waves do not. Coherent waves are produced by sources such as antennas, which emit energy through a collectively dependent process. Most electromagnetic waves produced by man-made devices at RF and microwave frequencies as we have been considering here are coherent. Coherency plays a key role in communications and remote-sensing applications of electromagnetic waves [51], since they enable different types of modulation. Lasers are an example of coherent wave sources at optical frequencies.

On the other hand, noncoherent waves result from the radiation of many collectively independent sources. In this case, the wave front is not well defined and random phase fluctuations occur across space (spatial incoherence) and with varying wavelengths at random intervals (temporal incoherence). Noncoherent sources include most natural sources of radiation such as the sun, light from fluorescent lamps and light bulbs, and LEDs.

In general, electromagnetic waves may exhibit some *partial* degree of coherence. As such, the classification into coherent and noncoherent waves corresponds to two ideal extremes.

9 RESEARCH CHALLENGES AND EMERGING APPLICATIONS

Electromagnetic wave propagation in simple media is now well understood from a theoretical standpoint; however, the propagation of electromagnetic waves in certain complex media such as manmade *metamaterials* is a topic of ongoing research interest. In addition, there are a number of applications that benefit from a more thorough understanding of the propagation of electromagnetic waves within natural media such as the troposphere and the ionosphere, which exhibit a combination of inhomogeneity, dispersion, and other effects. In this section, we very briefly consider these two applications.

9.1 Electromagnetic Wave Propagation in Metamaterials

Metamaterials are an umbrella term describing man-made materials exhibiting unusual properties not readily available in nature [52, 53]. One metamaterial example is double-negative (DNG) or left-hand (LH) media, that is, materials exhibiting *simultaneous* negative permittivity and permeability. The first discussion on the possibility of materials with simultaneous negative values of ε and μ appeared in [54]. Metamaterials are typically composed of very small cells, much smaller than the guided wavelength, which yield their exotic macroscopic constitutive parameters.

LH materials are so-called because the electric field, the magnetic field, and the phase constant vector of propagating waves form a left-handed triad instead of a right-hand (RH) triad as in ordinary media. This can be seen from a simple plane wave in homogeneous, lossless, and source-free region. From (21), with $\boldsymbol{k} = \boldsymbol{\beta}$:

$$\boldsymbol{E} = \boldsymbol{E}_o e^{-j\boldsymbol{\beta}\cdot\boldsymbol{r}} = \frac{1}{\omega\varepsilon}\boldsymbol{H}_o \times \boldsymbol{\beta} e^{-j\boldsymbol{\beta}\cdot\boldsymbol{r}} = \frac{1}{\omega\varepsilon}\boldsymbol{H} \times \boldsymbol{\beta} \tag{83}$$

$$\boldsymbol{H} = \boldsymbol{H}_o e^{-j\boldsymbol{\beta}\cdot\boldsymbol{r}} = \frac{1}{\omega\mu}\boldsymbol{\beta} \times \boldsymbol{E}_o e^{-j\boldsymbol{\beta}\cdot\boldsymbol{r}} = \frac{1}{\omega\mu}\boldsymbol{\beta} \times \boldsymbol{E} \tag{84}$$

Figure 10 Left-handed materials.

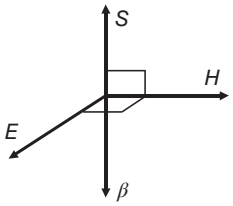

For a regular material where $\varepsilon > 0$ and $\mu > 0$, (83) and (84) indicate that $\boldsymbol{E}$, $\boldsymbol{H}$, and $\boldsymbol{\beta}$ form a triad according to the RH rule. But for double-negative materials, $\varepsilon < 0$ and $\mu < 0$, and therefore $\varepsilon = -|\varepsilon|$ and $\mu = -|\mu|$, leading to:

$$\boldsymbol{E} = -\frac{1}{\omega|\varepsilon|}\boldsymbol{H} \times \boldsymbol{\beta} \tag{85}$$

$$\boldsymbol{H} = -\frac{1}{\omega|\mu|}\boldsymbol{\beta} \times \boldsymbol{E} \tag{86}$$

In this case $\boldsymbol{E}$, $\boldsymbol{H}$, and $\boldsymbol{\beta}$ form a triad according to the LH rule, as shown in Fig. 10. In LH media, β and phase velocity are negative, as well as the refractive index, when compared to the positive direction given in RH media. Furthermore, it can be observed from Fig. 10 that the phase velocity ($\boldsymbol{\beta}$) is antiparallel to the power density ($\boldsymbol{S}$) and to the group velocity.

The boundary conditions at interfaces between two distinct media, given by (62), were directly obtained from Maxwell's equations and hold for both RH and LH media. But there is a qualitative difference for interfaces between RH and LH media. If no surface charge or current densities are present at the interface, the boundary conditions reduce to:

$$\begin{aligned} \boldsymbol{E_{1t}} &= \boldsymbol{E_{2t}} \;\; \varepsilon_1 E_{1n} = \varepsilon_2 E_{2n} \\ \boldsymbol{H_{1t}} &= \boldsymbol{H_{2t}} \;\; \mu_1 H_{1n} = \mu_2 H_{2n} \end{aligned} \tag{87}$$

which indicate the continuity of tangential electric and magnetic fields at the interface. On the other hand, the normal components of $\boldsymbol{E}$ and $\boldsymbol{H}$ are discontinuous. When both media are RH ($\varepsilon_1 > 0$, $\mu_1 > 0$, $\varepsilon_2 > 0$, $\mu_2 > 0$), the normal components of $\boldsymbol{E}$ and $\boldsymbol{H}$ point in the same direction. On the other hand, if medium 1 is RH ($\varepsilon_1 > 0$, $\mu_1 > 0$) and medium 2 is LH ($\varepsilon_2 < 0$, $\mu_2 < 0$), the normal components of $\boldsymbol{E}$ and $\boldsymbol{H}$ differ not only in magnitude but also present opposite direction to each other:

$$E_{1n} = -\frac{|\varepsilon_2|}{\varepsilon_1}E_{2n} \qquad H_{1n} = -\frac{|\mu_2|}{\mu_1}H_{2n} \tag{88}$$

Similarly, when plane waves are incident from an RH medium (medium 1) to an LH medium (medium 2), as in Fig. 3, the continuity of the tangential components of the electric and magnetic fields requires the phase matching along the interface, resulting in Snell's law (67), as for an RH–RH interface. But if medium 2 is LH, its refraction index is negative, $n_2 = -|n_2|$, and therefore Snell's law becomes:

$$n_1 \sin\theta_\mathrm{i} = -|n_2| \sin\theta_\mathrm{t} \tag{89}$$

This condition is satisfied for negative transmission angle $\theta_\mathrm{t} = -\theta_2$, as shown in Fig. 11. This is called a negative refraction, corresponding to a negative refraction angle θ_t:

$$\sin\theta_2 = -\sin\theta_\mathrm{t} = \frac{n_1}{|n_2|}\sin\theta_\mathrm{i} \tag{90}$$

In addition to LH media, another important class of metamaterials designed for the control of electromagnetic wave propagation are those obtained by *transformation optics* (TO) techniques. TO techniques rely on the interesting fact that the form of Maxwell's equations is invariant with respect to deformations on the metric of space [55].

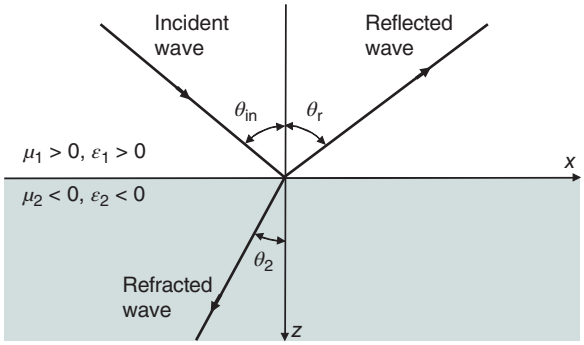

Figure 11 Negative refraction: Plane-wave incidence on a plane interface from a RH to a LH medium.

This can be summarily explained as follows. Let us assume Maxwell's equations in a spatial domain with parameters ε and μ represented by spatial coordinates (x, y, z). If the coordinates (x, y, z) are mapped (deformed) to coordinates (x', y', z') (together with the respective field solutions), then Maxwell's equations (together with the new, "deformed" solutions) can be referred back to the original coordinates (x, y, z) but now in an effective, doubly anisotropic medium (TO-designed metamaterial) [56]. It can be shown that the constitutive properties of such effective medium depend on the Jacobian of the coordinate transformation. This form invariance is explicitly manifested when Maxwell's equations are written based on the exterior calculus of differential forms [57–59]. Research interest in TO became very strong since 2006 when it was theoretically demonstrated that an object could coated by a TO-based cloaking metamaterial in such a way that no scattered field would be produced given a narrowband but otherwise arbitrary incident electromagnetic wave. This would effectively render the coated object "invisible" to incoming radiation [60]. Later, other TO-based metamaterial devices were proposed such as "masking" [61], "mirage" [62], and generalized impedance matched [63] devices.

Despite many interesting properties and myriad possible applications of metamaterials, their fabrication is not a simple task. Popular approaches involve the combination of an array of thin wires (TW) and split-ring resonators (SRR), as shown in Fig. 12, or other structured cells [64–66]. The TW array can provide the permittivity response while the SRRs can provide the permeability response. In the case of LH media, for example, such configuration behave as desired if the incident wave has the electric field parallel to the wires, and the magnetic field orthogonal to the SRRs. For TO media, spatial inhomogeneity is often a necessary property which means that the cell sizes and/or orientations need to vary across the structure [67]. Typically, the average cell size should remain smaller than about one quarter of the wavelength so that an effective medium description is valid.

9.2 Electromagnetic Wave Propagation Effects in the Troposphere and Ionosphere

The modeling and prediction of propagation effects in the troposphere and ionosphere are important in a number of applications. The troposphere can be approximated as a dielectric media with stratified properties where the refractive index n varies with height. Such stratification cause refraction of the wave (or bending of the rays in the GO description). The refractive index n also exhibits geographical changes due to local variations on temperature, pressure, and humidity. Tropospheric effects influence point-to-point and point-to-area wireless communication links near the ground as well as satellite communications, radar, and remote-sensing systems in general [36]. The troposphere is a frequency-dispersive medium that exhibits frequency- and time-dependent propagation losses. Stronger propagation losses in the troposphere are typically associated to the effect of atmospheric gases or to the presence of hydrometeors in the propagation path [12]. These losses need to be properly taken into account for the design of wireless communications and radars. The ionosphere on the other hand also influences satellite communication links as well as the so-called skywave communication links that rely on reflections from ionospheric layers to establish communications between two far apart stations in the ground. In addition to attenuation effects, the ionosphere may perturb the polarization of certain signals (in a frequency-dependent manner) due

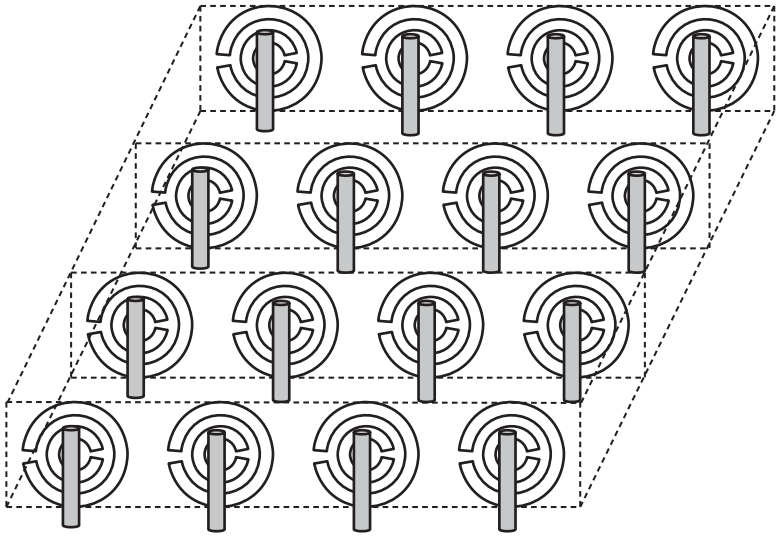

Figure 12 Metamaterial structure made of a periodic arrangement of thin-wires and split-ring resonators.

to a phenomenon called Faraday rotation [12]. Both the troposphere and the ionosphere also cause scintillation effects, which are relatively fast variations on the received signal amplitude due to time-varying refraction effects and inhomogeneities present along the propagation path. Finally, the troposphere and the ionosphere also cause perturbations on the phase and group delay and other parameters measured by global navigation satellite systems (GNSS) such as GPS, thus, affecting their positioning accuracy [68]. More details about tropospheric and ionospheric propagation effects are given in [12]. Ongoing research efforts seek to measure, model, monitor, and forecast such effects [69–71].

10 CLASSICAL VERSUS QUANTUM REGIME AND FINAL REMARKS

Maxwell's equations in their classical form are invariant to Lorentz transformations [72] and compatible with special relativity. Indeed, the need to preserve the form of Maxwell's equations in any nonaccelerated frames of reference (special relativity principle) was one of the major drives for the development of the theory of special relativity by Einstein [73].

In this chapter we have focused mainly on aspects of electromagnetic wave propagation in simple media at the classical physics level. For the vast majority of RF and microwave applications, this classical description is sufficient. However, some details of the interaction and propagation of electromagnetic waves in material media at the molecular and atomic levels depends on quantum aspects that are not captured by a strict classical description. In the quantum description, electromagnetic fields are elevated from vector *functions* to *operators* acting on quantum state vectors in a Hilbert space (state space). The theory of electromagnetic interaction that takes into account the laws of both relativity and quantum mechanics is called quantum electrodynamics (QED) [74, 75]. The development of QED was the basis for the 1965 Nobel Prize in physics, shared by Tomonaga (1906–1979), Schwinger (1918–1994), and Feynmann (1918–1988), who followed earlier developments by Dirac (1902–1984). At low energies and when averaged at the macroscopic level, QED reduces to Maxwell's equations augmented by phenomenological equations that can be expressed in terms of the macroscopic constitutive laws discussed in this chapter.

BIBLIOGRAPHY

1 J. C. Maxwell, *Electricity and Magnetism*, Academic Press, NY, 1935.
2 M. Born and E. Wolf, *Principles of Optics*, 6th ed., Pergamon Press, Oxford, 1980.
3 R. S. Elliott, *Electromagnetics: History, Theory, and Applications*, IEEE Press, Piscataway, NJ, 1993.
4 J. D. Jackson, *Classical Electrodynamics*, 3rd ed., Wiley, NY, 1999.
5 J. A. Stratton, *Electromagnetic Theory*, McGraw-Hill Book Co., NY, 1941.
6 R. F. Harrington, *Time-Harmonic Electromagnetic Fields*, McGraw-Hill Book Co., NY, 1961.
7 R. E. Collin, *Field Theory of Guided Waves*, 2nd ed., IEEE Press, Piscataway, NJ, 1991.
8 L. B. Felsen and N. Marcuvitz, *Radiation and Scattering of Waves*, IEEE Press, Piscataway, NJ, 1994.
9 S. Silver, ed., *Microwave Antenna Theory and Design*, McGraw-Hill Book Co., NY, 1949.
10 J. A. Kong, *Electromagnetic Wave Theory*, EMW Publishing, Cambridge, MA, 2000.
11 W. Chew, *Waves and Fields in Inhomogeneous Media*, IEEE Press, Piscataway, NJ, 1995.
12 C. A. Levis, J. T. Johnson, and F. L. Teixeira, *Radiowave Propagation: Physics and Applications*, Wiley, NY, 2010.
13 Cross reference for *Maxwell's Equations* in the *Wiley Encyclopedia of RF and Microwave Engineering*.
14 P. M. Morse and H. Feshbach, *Methods of Theoretical Physics*, Vol. 1, McGraw-Hill Book Co., NY, 1953.
15 A. Taflove and S. C. Hagness, *Computational Electrodynamics: The Finite-Difference Time-Domain Method*, 3rd ed., Artech House, Boston, 2005.
16 F. L. Teixeira, Time-domain finite-difference and finite-element methods for Maxwell equations in complex media, *IEEE Trans. Antennas Propagat.* 56(8): 2150–2166 (2008).
17 R. F. Harrington, *Field Computation by Moment Methods*, Wiley-IEEE Press, Piscataway, NJ, 1993.
18 P. C. Clemmow and J. Wait, *The Plane Wave Spectrum Representation of Electromagnetic Fields*, Oxford Univ. Press, UK, 1996.
19 C. A. Balanis, *Antenna Theory: Analysis and Design*, 4th ed., Wiley, NY, 2016.
20 G. A. Deschamps, Ray Techniques in Electromagnetics, *Proc. IEEE* 60(9): 1022–1035 (Sep. 1972).
21 D. E. Kerr, ed., *Propagation of Short Radio Waves*, McGraw-Hill Book Co., NY, 1949.
22 J. D. Parsons, *The Mobile Radio Propagation Channel*, 2nd ed., Wiley, NY, 2000.
23 A. Yariv and P. Yeh, *Optical Waves in Crystals*, Wiley, NY, 1984.
24 K.-Y. Jung, B. Donderici, and F. L. Teixeira, Transient analysis of spectrally asymmetric magnetic photonic crystals with ferromagnetic losses, *Phys. Rev. A* 74: 165207 (2006).
25 A. Figotin and I. Vitebskiy, Nonreciprocal magnetic photonic crystals, *Phys. Rev. E* 63: 066609 (2001).
26 K.-Y. Jung and F. L. Teixeira, Numerical study of photonic crystals with a split band edge: polarization dependence and sensitivity analysis, *Phys. Rev. A* 78: 043826 (2008).
27 M. Oristaglio and B. Spies, eds., *Three-dimensional Electromagnetics*, Society of Exploration Geophysicists, Tulsa, OK, 1999.
28 H. O. Lee and F. L. Teixeira, Cylindrical FDTD analysis of LWD tools through anisotropic dipping-layered earth media, *IEEE Trans. Geosci. Remote Sens.* 45(2): 383–388 (2007).
29 H. Moon, B. Donderici, and F. L. Teixeira, Stable evaluation of Green's functions in cylindrically stratified regions with uniaxial anisotropic layers, *J. Comp. Phys.* 325: 174–200 (2016).
30 R. A. Chilton, K. Jung, R. Lee, and F. L. Teixeira, Frozen modes in parallel-plate waveguides loaded with magnetic photonic crystals, *IEEE Trans. Microwave Theory Tech.* 55(12): 2631–2641 (2007).
31 A. Figotin and I. Vitebskiy, Slow wave phenomena in photonic crystals, *Laser Photonics Rev.* 5(2): 201–213 (2011).
32 C. A. Balanis, *Advanced Engineering Electromagnetics*, 2nd ed., Wiley, NY, 2012.
33 D. K. Cheng, *Field and Wave Electromagnetics*, 2nd ed., Addison-Wesley Pub. Co., Reading, MA, 1992.
34 D. M. Pozar, *Microwave Engineering*, 4th ed., Wiley, NY, 2012.

35 S. Ramo, J. R. Whinnery, and T. Van Duzer, *Field and Waves in Communication Electronics*, 2nd ed., Wiley, NY, 1984.

36 H. L. Bertoni, *Radio Propagation for Modern Wireless Systems*, Prentice-hall, NY, 2000.

37 J. A. Buck, *Fundamentals of Optical Fibers*, Wiley, NY, 1995.

38 F. L. Teixeira, ed., *Geometric Methods for Computational Electromagnetics*, EMW Publishing, Cambridge, MA, 2001.

39 J. J.-H. Wang, *Generalized Moment Methods in Electromagnetics*, Wiley, NY, 1991.

40 U. C. Resende, F. J. S. Moreira, and O. M. C. Pereira-Filho, EMFIE and MEFIE formulations for the analysis of scattering from dielectric and composite bodies of revolution, *Microwave Opt. Tech. Lett.* 53: 398–402 (2011).

41 J. Jin, *The Finite Element Method in Electromagnetics*, 2nd ed., Wiley, NY, 2002.

42 D. A. McNamara, C. W. I. Pistorius, and J. A. G. Malherbe, *Introduction to the Uniform Geometrical Theory of Diffraction*, Artech House, NY, 1990.

43 D. N. Schettino, F. J. S. Moreira, K. L. Borges, and C. G. Rego, Novel heuristic UTD coefficients for the characterization of radio channels, *IEEE Trans. Magn.* 43: 1301–1304 (2007).

44 D. N. Schettino, F. J. S. Moreira, and C. G. Rego, Efficient ray tracing for radio channel characterization of urban scenarios, *IEEE Trans. Magn.* 43: 1305–1308 (2007).

45 Cross reference for Transmission Lines in *Wiley Encyclopedia of RF and Microwave Engineering*.

46 G. Keiser, *Optical Fiber Communications*, 3rd ed., McGraw-Hill, NY, 2000.

47 L. A. Fonseca and H. E. Hernandez-Figueroa, Full-wave interior penalty discontinuous Galerkin method for waveguide analysis, *J. Lightwave Technol.* 36: 5168–5176 (2018).

48 G. S. Rosa, J. R. Bergmann, and F. L. Teixeira, A robust mode-matching algorithm for the analysis of triaxial well-logging tools in anisotropic geophysical formations, *IEEE Trans. Geosci. Remote Sens.* 55(5): 2534–2545 (2017).

49 G. S. Rosa, M. S. Canabarro, J. R. Bergmann, and F. L. Teixeira, A comparison of two numerical mode-matching methodologies for the analysis of inhomogeneous media with radial and vertical stratifications, *IEEE Trans. Antennas Propagat.* 66: 7499–7504 (2018).

50 G. S. Rosa, J. R. Bergmann, and F. L. Teixeira, A perturbation method to model electromagnetic well-logging tools in curved boreholes, *IEEE Trans. Geosci. Remote Sens.* 56: 1979–1993 (2018).

51 M. E. Yavuz and F. L. Teixeira, *Time Reversal Based Signal Processing Techniques: Algorithms and Applications on Ultrawideband Electromagnetic Remote Sensing*, VDM Verlag, Germany, 2009.

52 G. Eleftheriades and K. G. Balmain, *Negative-Refraction Metamaterials*, IEEE Press, John Wiley & Sons, NJ, 2005.

53 C. Caloz and T. Itoh, *Electromagnetic Metamaterials*, IEEE Press, John Wiley & Sons, NJ, 2006.

54 V. Veselago, The electrodynamics of substances with simultaneously negative values of ϵ and μ, *Soviet Physics Uspekhi* 10(4): 509–514 (1968).

55 F. L. Teixeira and W. C. Chew, Differential forms, metrics, and the reflectionless absorption of electromagnetic waves, *J. Electromag. Waves Appl.* 13: 665–686 (1999).

56 F. L. Teixeira and W. C. Chew, Lattice electromagnetic theory from a topological viewpoint, *J. Math. Phy.* 40(1): 169–187 (1999).

57 G. A. Deschamps, Electromagnetics and differential forms, *Proc. IEEE* 69: 676–696 (1981).

58 K. F. Warnick, R. H. Selfridge, and D. V. Arnold, Teaching electromagnetic field theory using differential forms, *IEEE Trans. Edu.* 40: 53–68 (1997).

59 F. L. Teixeira, Differential form approach to the analysis of electromagnetic cloaking and masking, *Microwave Opt. Tech. Lett.* 49(8): 2051–2053 (2007).

60 J. B. Pendry, D. Schurig, and D. R. Smith, Controlling electromagnetic fields, *Science* 312: 1780–1782 (2006).

61 F. L. Teixeira, Closed-form metamaterial blueprints for electromagnetic masking of arbitrarily-shaped convex PEC objects, *IEEE Antennas Wireless Propagat. Lett.* 6: 163–164 (2007).

62 A. Diatta, G. Dupont, S. Guenneau, and S. Enoch, Broadband cloaking and mirages with flying carpets, *Opt. Express* 18: 11537–11551 (2010).

63 B. Donderici and F. L. Teixeira, Metamaterial blueprints for reflectionless waveguide bends, *IEEE Microwave Wireless Compon. Lett.* 18(4): 233–235 (2008).

64 H. Odabasi, F. L. Teixeira, and D. O. Guney, Electrically small, complementary electric-field-coupled resonator antennas, *J. Appl. Phys.* 113: 084903 (2013).

65 H. Jeong, T. T. Nguyen, and S. Lim, Subwavelength metamaterial unit cell for low-frequency electromagnetic absorber applications, *Sci. Reports* 8: 16774 (2018).

66 H. Odabasi and F. L. Teixeira, Electric-field coupled resonators as metamaterial loadings for waveguide miniaturization, *J. Appl. Phys.* 114: 214901 (2013).

67 H. F. Ma and T. J. Cui, Three-dimensional broadband ground-plane cloak made of metamaterials, *Nature Comm.* 1: 21 (2010).

68 T. H. Kindervatter and F. L. Teixeira, *Tropospheric and Ionopsheric Effects on Global Navigation Satellite Systems*, Wiley-IEEE Press, NJ, 2022.

69 P. Yu, I. A. Glover, P. A. Watson, O. T. Davies, S. Ventouras, and C. Wrench, Review and comparison of tropospheric scintillation prediction models for satellite communications, *Int. J. Satellite Comm. Networking* 24: 283–302 (2006).

70 A. S. Rodger and M. J. Jarvis, Ionospheric research 50 years ago, today and tomorrow, *J. Atmospheric Solar-Terrestrial Phys.* 62: 1629–1645 (2000).

71 S. M. Radicella and B. Nava, Chapter 6 - Empirical ionospheric models, in M. Materassi, B. Forte, A. J. Coster, and S. Skone, eds., *The Dynamical Ionosphere*, Elsevier, The Netherlands, 2020.

72 C. W. Misner, K. S. Thorne, and J. A. Wheeler, *Gravitation*, W. H. Freeman, San Fransisco, 1973.

73 A. Einstein and L. Infeld, *Evolution of Physics*, Simon and Schuster, New York, 1966.

74 V. B. Berestetskii, E. M. Lifshitz, and L. P. Pitaevskii, *Quantum Electrodynamics*, 2nd ed., Pergamon Press, Oxford, 1982.

75 J. Schwinger, ed., *Selected Papers on Quantum Electrodynamics*, Dover, New York, 1958.